

I give permission for public access to my thesis and for copying to be done at the discretion of the archives' librarian and/or the College library.

---

Signature

---

Date

**Regulation of *Matrix Metalloproteinase 2* Expression by *E93* during Fat Body  
Remodeling in *Drosophila melanogaster***

By Nshunge Musheshe

A Paper Presented to the Faculty of  
Mount Holyoke College in  
Partial Fulfillment of the Requirements for  
The Degree of Bachelors of Arts with  
Honor

Department of Biological Sciences  
South Hadley, MA 01075

May 2012

This paper was prepared  
under the direction of  
Professor Craig Woodard  
for eight credits

This is a dedication to my family (my biggest fans) for giving me smiles, for continuously allowing me to explore my potential, and most of all for loving me and for always showing it


---I would not have done it without you 😊😊😊😊

A mini dedication to my laptop too, for not giving up on me.

## ACKNOWLEDGEMENTS

My answer is always the same when someone asks, “Why Mount Holyoke College? Or why U.S.A for school? ” With my head high, and my famous smile, I say, “It is all a leap of faith”. This same phenomenon got me walking into Professor Craig Woodard’s lab, my adviser, one random morning, and I asked to be a student researcher in his lab: with no intentions of writing a thesis of course. But then again ‘another leap of faith’ and now you have one to read from me.

I would love to thank Professor Craig Woodard for mentoring me, and shaping me into a passionate researcher. My experiences in the lab have been quite challenging but with continuous and unconditional support from Craig. The laughs and hi-fives after every successful experiment made me love my research more. Thank you so much Craig.

I would like to thank Professor Eric Baehrecke of University of Massachusetts, school of Medicine, for providing me with the fly stocks that I used for my research. Thanks to my labmates for making the fly food so that my stocks would be healthy and in shape for my research, and most importantly for sharing their knowledge about the ‘most wanted animal in the lab’-‘*Drosophila melanogaster*’ . Special thanks to Jennifer Ty for patiently conducting some of the experiments with me and for making it a fun process.

Thanks to my dearest friends and all my professors for making Mount Holyoke feel like home away from home, and also for believing in me. Special thanks to Abena Kwaa and Loretah Chibaya for the moral support and for encouraging me during the early stages of my writing.

Of course, all this would not have been possible without my amazing support team that always gives me positive energy through thick and thin; my parents (Prossy and Mwalimu), and my siblings (Tatra, Nchume and Bliika), Dana and Curtis, Alida and Reint, Judy Murdock, Martha and Don, , The Willetts, Silvana, and all family friends. Thank you for allowing me to experience Mount Holyoke and every opportunity that has come my way to the fullest. I know I have put off medical school for quite some time but then again ‘another leap of faith?’ I will get there--maybe not this year but in a few for sure ☺. I LOVE YOU.

## TABLE OF CONTENTS

ACKNOWLEDGEMENTS.....	ii
INTRODUCTION.....	1
The life cycle of <i>Drosophila melanogaster</i> .....	4
Matrix metalloproteinases (MMPs).....	6
Biochemistry of MMP2 .....	8
<i>Drosophila Timp</i> (Tissue Inhibitor of Metallo-Proteases) Inhibits both <i>MMP1</i> and <i>MMP2</i> .....	10
Remodeling of the fat body .....	11
Steroid Hormones .....	14
Steroid Hormones in <i>Drosophila</i> .....	15
20E.....	17
E93.....	21
Biochemistry of E93 protein .....	23
MATERIALS AND METHODS.....	27
Stocks and Crosses.....	27
RNA Isolation.....	28
cDNA Synthesis .....	30
Primer Design.....	32
Reverse Transcription Polymerase Chain Reaction (RT-PCR) .....	33
Gel Electrophoresis .....	35
Primer Optimization.....	36
Calculation of Primer Efficiency .....	42
Experimental qPCR.....	44
Calculation of fold change in qPCR .....	45
RESULTS .....	48
Confirmation of the role of <i>E93</i> in fat body remodeling .....	48
Confirmation of <i>MMP2</i> expression using RT-PCR.....	48
Primer efficiencies in qPCR .....	50
Expression of <i>MMP2</i> in <i>E93<sup>1</sup>/Df(3R)93F<sup>X2</sup></i> at 10 hours APF.....	53

DISCUSSION .....	55
Expression of <i>MMP2</i> in the Fat Body of <i>w<sup>1118</sup></i> and <i>E93<sup>1</sup>/Df(3R)93F<sup>x2</sup></i> at 10 hours APF	55
Implications of Downregulation and Upregulation of <i>MMP2</i> .....	56
Future studies of MMPs and E93 in <i>Drosophila</i> .....	58
Transmission Electron Microscopy .....	58
SOURCES OF ERROR IN THE EXPERIMENT .....	61
APPENDIX .....	62
Abbreviations used .....	62
REFERENCES.....	67

## LIST OF FIGURES

Figure 1. The Complete Life Cycle of <i>Drosophila melanogaster</i> .....	5
Figure 2. Important Structural Features of MMP2 .....	9
Figure 3: Retraction, Disaggregation and Detachment Stages During Fat Body Remodeling in <i>Drosophila melanogaster</i> .....	13
Figure 4. Major Life Developmental Stages of <i>Drosophila melanogaster</i> .....	18
Figure 5. Premature Expression of $\beta$ ftz-f1 During Fat Body Remodeling in <i>Drosophila</i> <i>melanogaster</i> .....	20
Figure 7. Genes Expressed as a Response to 20E Signaling .....	25
Figure 8. Dissociation Curve for <i>MMP2</i> .....	41
Figure 9. Standard Curve Generated to Calculate Primer Efficiency of <i>MMP2</i> Primers at 10hrs APF of control (w1118) cDNA .....	43
Figure 10. 1.6% Ethidium Bromide-Stained Agarose Gel.....	49
Figure 11. Relative Expression of <i>MMP2</i> in $E93^1/Df(3R)93F^{X2}$ .....	53
Figure 12. Exponential curves for the different dilutions ranging from 0.026ng to 260ng of $w^{1118}$ cDNA at 10 hours APF with <i>Actin 5C</i> primer set generated in the 7300 BioAnalyzer software. ....	65
Figure 13. Exponential curves for each w1118 cDNA dilution (ranging from 0.026ng to 260ng) at 10 hours APF.....	66



## LIST OF TABLES

Table 1. Pipetting Scheme for One cDNA Synthesis Reaction .....	31
Table 2. Pipetting Scheme for the Second Master Mix for cDNA Synthesis .....	31
Table 3. Preparation of Master Mix Reactions for RT-PCR .....	34
Table 4. Temperature Profile for the Tech Techgene Thermocycler for RT-PCR.....	35
Table 5: Pipetting Scheme for qPCR .....	38
Table 6: Cycles of qPCR .....	39
Table 7. Annealing Temperatures for <i>MMP2</i> and <i>Actin 5C</i> Primers used in the Instrument Set-up.....	50
Table 8. Primer set concentrations for endogenous gene and target genes used.....	51
Table 9. Primer Efficiencies Obtained from Standard Curves.....	51
Table 10. $\Delta C_t$ values of the control ( $w^{1118}$ ) and $E93^1/Df(3R)93F^{x2}$ obtained from Experimental qPCR. ....	52
Table 11. A sample 96-well plate layout that was used for primer concentration optimization.....	63
Table 12. A sample 96-well plate layout that was used to obtain validation primer efficiencies .....	63
Table 13. A sample 96-well plate layout for the Experimental qPCR to determine gene expressions at 10 hours APF .....	64

## ABSTRACT

Changes in *Drosophila melanogaster* occur as the larva undergoes a complete transformation during metamorphosis to give rise to the adult. During this transformation some larval tissues are destroyed while other larval tissues such as the fat body which is involved in fueling metamorphosis undergo proliferation and differentiation.

The steroid-regulated gene, *E93*, plays an important role in larval salivary gland and midgut programmed cell death early in metamorphosis. *E93* protein is bound to the sites of steroid-regulated genes and cell death genes on polytene chromosomes. *E93* mutants possess larval salivary glands that fail to undergo steroid-triggered programmed cell death. This indicates that *E93* may control the pupal-specific responses of many target genes since it is required for preformation at the pupal stage.

It has been shown that the remodeling of the fat body in *Drosophila melanogaster* requires expression of *Matrix metalloproteinase 2 (MMP2)*, presumably to break down the extracellular matrix (ECM) holding the tissue together. The remodeling of the larval fat body takes place during early metamorphosis and it involves the dissociation of the tissue of closely associated polygonal cells into individualized spherical cells. Fat body remodeling is divided into three stages: retraction, disaggregation, and detachment. The detachment phase of fat body remodeling occurs concurrently with expression of *MMP2* during the prepupal to pupal transition stage.

Past research has shown that ecdysone signaling cascades are required for fat body remodeling. During the second pulse of 20E (the most active form of ecdysone) during the prepupal-pupal transition stage, both *E93* and *MMP2* are expressed. In my research I examine *E93* loss-of-function mutants and wild type for expression of *MMP2* transcripts in fat body to test the hypothesis that *E93* regulates transcription levels of *MMP2* during fat body remodeling in *Drosophila melanogaster*.

## INTRODUCTION

Programmed cell death is important for normal development and maintenance of homeostasis, and it is required to ensure host defense against pathogens in animals (Jacobsen et al., 1997, Vaux and Korsmeyer, 1999). Programmed cell death differs from necrotic cell death because it does not lead to an inflammatory response but instead it is genetically regulated (Lockshin and Zakeri 1991).

A detailed study of programmed cell death is necessary, and this is because the misregulation of programmed cell death usually results in devastating consequences that include, but are not limited to, tumorigenesis, autoimmune diseases, and neurodegenerative diseases (Krammer., 2000; Yuan and Yankner., 2000). There are two forms of programmed cell death and these include: apoptosis and autophagy.

Apoptosis and autophagy are morphologically distinct even though they are both forms of programmed cell death. Apoptosis is usually observed in isolated dying cells which are characterized by nuclear and cytoplasmic condensation. Apoptosis leads to change in morphology of the cells. These changes include: decrease in the size of cells, and chromosomal DNA fragmentation, among others.

During apoptosis, the cell fragments known as apoptotic bodies that are produced, engulf other cells and prevent them from causing damage to neighboring tissues. Unlike necrosis which is a detrimental form of cell death, apoptosis is required for normal development during the life cycle of an organism. For example; in humans, apoptosis is required for the individualized differentiation of fingers and toes during embryonic development.

At low levels of apoptosis, there is limited cell death and this may result in cancer and autoimmune diseases due to the accumulation of cells. Extreme apoptosis however, entails uncontrolled cell death, which may progress into neurodegenerative diseases, and tissue damage, among others. Apoptosis has also been implicated in Human Immunodeficiency Virus (HIV) progression to AIDS. In the event of an infection with HIV, the virus attacks the CD4+ T-helper cells which are required for the immune response.

The Cd4+ T-helper cells are rapidly reduced in number to suppress the immune system, and therefore a limited amount of markers for apoptosis is available. This in turn gives the virus ample time to continue releasing virions and agents for apoptosis. The biochemical mechanism by which these CD4+ T-helper cells are destroyed is greatly enhanced by apoptosis (Alimonti, B et al., 2003).

Autophagy on the other hand, is frequently observed when a group of cells or an entire tissue dies. Autophagy occurs during development of diverse organisms, and it has been associated with tumorigenesis. Autophagy also plays a

role in homeostasis and cell growth, and it involves separation of the targeted cell from the rest of the cytoplasm by creating a membrane around the cell. The resultant vesicle formed then fuses with a lysosome which degrades its contents.

This mechanism of autophagy may contribute to prevention of disease processes like cancer, and also contribute to the release of nutrients during starvation of an organism by breaking down non-vital components (Yorimitsu T and Klionsky DJ, 2005). Steroid-activated programmed cell death of the *Drosophila melanogaster* salivary glands occurs by autophagy (Lee and Baehrecke., 2001).

Changes in *Drosophila melanogaster* occur as the larva undergoes a complete transformation during metamorphosis to give rise to the adult. Metamorphosis refers to the complete change in form and physical appearance of the insect. Steroid hormones have been identified as necessary regulators of programmed cell death.

Metamorphosis begins to occur in response to a pulse of 20-hydroxyecdysone (20E)- the most active form of ecdysone, and during this transformation some larval tissues such as the salivary glands are destroyed, while other larval tissues, such as the fat body which is involved in fueling metamorphosis, undergo proliferation and differentiation (Bainbridge and Bownes, 1981).

## **The life cycle of *Drosophila melanogaster***

The life cycle of *Drosophila* is divided into four major stages; the embryo, larva, pupa and adult (Figure 1). The larval stage is divided into three instars during which the larva feeds and grows in size. After each of the first two instars, the larva undergoes a molt. Embryonic development occurs during the first 24 hours of life. The 1<sup>st</sup> and 2<sup>nd</sup> larval instars are each completed in one day, while the 3<sup>rd</sup> larval instar lasts for two days.

Once feeding stops, the 3<sup>rd</sup> larval instar begins to search for a location in which to start metamorphosis. On arrival in the favorable location, the 3<sup>rd</sup> larval instar pupariates to become a prepupa. Pupariation, or puparium formation, is the beginning of metamorphosis, and at this time the age of the animal is referred to as 0 hours After Puparium Formation (APF). The complete life cycle of a *Drosophila* takes a total of about nine days at 25°C (Page McCaw et al., 2003).

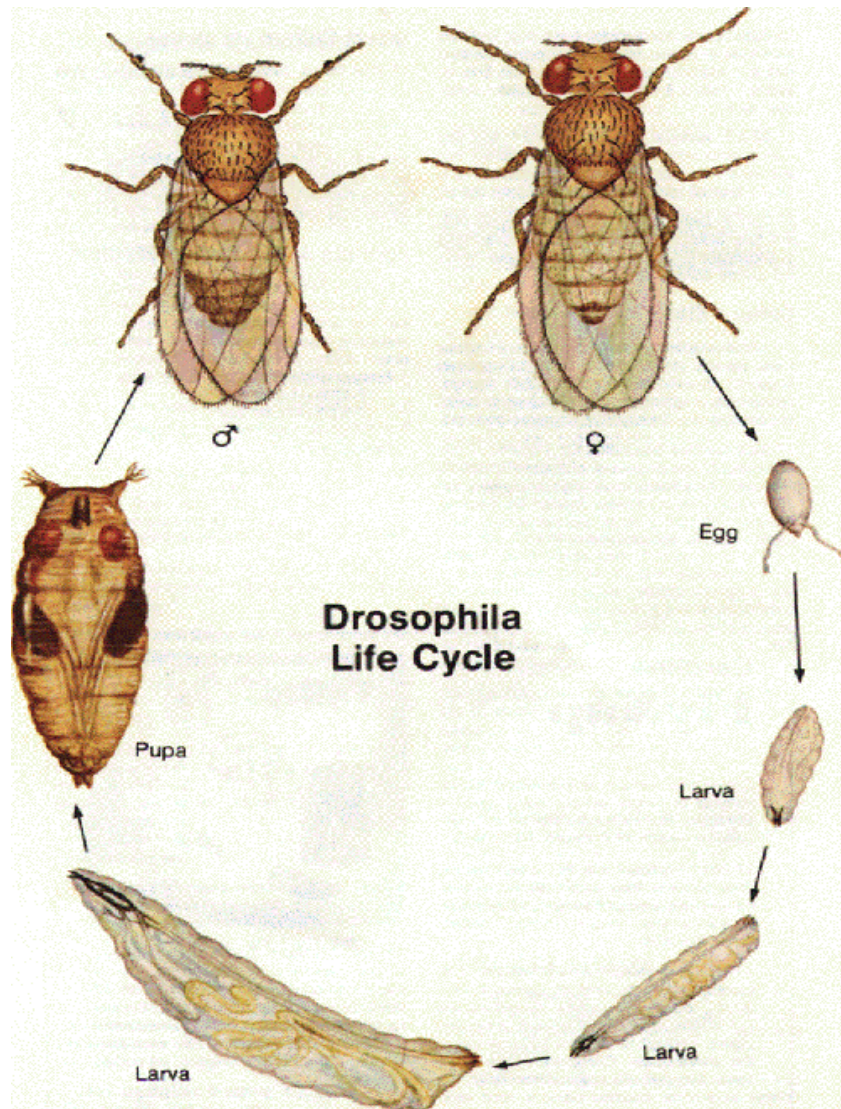


**Figure 1. The Complete Life Cycle of *Drosophila melanogaster*.** (Figure from Carolina Drosophila manual - (Carolina Biology Supply, 2700 York Road, Burlington North Carolina).

## **Matrix metalloproteinases (MMPs)**

**Matrix metalloproteinases** (MMPs) are a family of enzymes that can cleave almost all protein components of the Extra Cellular Matrix (ECM). MMPs are believed to be responsible for both normal and disease processes such as cancer. The ECM is a complex network of proteins and proteoglycans that is involved in cell adhesion, cell signaling, and structural maintenance of tissues (Page McCaw et al., 2003).

In addition to providing support to the tissues, the ECM regulates intercellular communication. The ECM must be altered in order for normal events of embryogenesis, metamorphosis, tissue remodeling, or cell migration through barriers to occur. The ECM is also degraded during the course of many diseases such as cancer growth and metastasis (Page McCaw et al., 2003). There are more than 20 MMPs in mammals which share similar substrate specificities with one another (McCawley and Matrisian, 2001; Sternlicht and Werb, 2001).

The *Drosophila* genome contains two genes that encode MMPs. After studying MMP function during development of the fruitfly, *Drosophila melanogaster*, it has been learned that neither MMP type whether in mammals or in the fruitfly is required for embryogenesis, but rather MMPs are required for later developmental remodeling (Page McCaw et al., 2003).



*D. melanogaster* has two MMPs; MMP1 and MMP2 (Llano et al., 2000, 2002; Page-McCaw et al., 2003). MMP1 is a secreted protein, and MMP2 has a GPI anchor and therefore is membrane associated (Llano et al., 2002; Page-McCaw et al., 2003). The two *D. melanogaster* MMPs have the canonical MMP structure but are not orthologs of any of the 24 mammalian MMPs (Page-McCaw et al., 2003).

*MMP1* and *MMP2* are each required for distinct aspects of tissue remodeling and programmed cell-death during metamorphosis (Page-McCaw et al., 2003). *MMP1* is required for larval tracheal growth and events of pupal morphogenesis while *MMP2* is required during metamorphosis and is explicitly involved in histolysis of larval tissues and epithelial fusion (Page McCaw et al., 2003).

Larval tissue histolysis and metamorphosis in *Drosophila* are controlled by hormonal regulation and therefore are triggered by a response to the ecdysone steroid hormone-20-Hydroxyecdysone (20E). Before head eversion, the wing discs fuse along the midline of the nodum early in morphogenesis and *MMP2* has been shown to play a role in this process.

In *Drosophila*, *MMP2* is required for fat body remodeling and is also sufficient to induce fat body remodeling. By prematurely expressing *MMP2*, fat body remodeling was prematurely induced and this provided proof that *MMP2* is required for fat body remodeling (Bond et al., 2011).

The major function of *MMP2* is degradation of ECM by proteolytically digesting gelatin and other types of collagen which include; types IV, V, VII, IX and X that make up the ECM. *MMP2* successfully degrades collagen IV, thereby assisting in migration of metastatic cancer cells through the basement membrane.

*MMP2* in humans together with other MMPs facilitates tumor progression by degrading the interstitial connective tissue and basement membranes of the ECM. *MMP2* and *MMP-9* are found to be elevated in invasive cancers such as breast cancer and oral cancer, among others (Egeblad and Werb, 2002). But also, *MMP2* in conjunction with other MMPs is required for tissue remodeling events such as ovulation, wound healing and embryonic development in mammals.

## **Biochemistry of MMP2**

*MMP2* in *Drosophila melanogaster* is located at the cytological region 46A. *MMP2* has a conventional MMP structure. It has a catalytic domain, a C-terminal hemopexin domain that binds substrates and inhibitors, an N-terminal pro domain that maintains an inactive zymogen state which is cleaved to activate the protease, and a signal sequence.

Unlike *MMP1*, the *MMP2* hinge domain contains a cluster of eight repeats of the sequence RRRQEEE and four more of a closely related sequence, which is

not found in any other MMP family members, and this sequence has an unknown function (Page McCaw et al., 2003). A basic structural composition of MMP2 and its domains is shown in Figure 2.

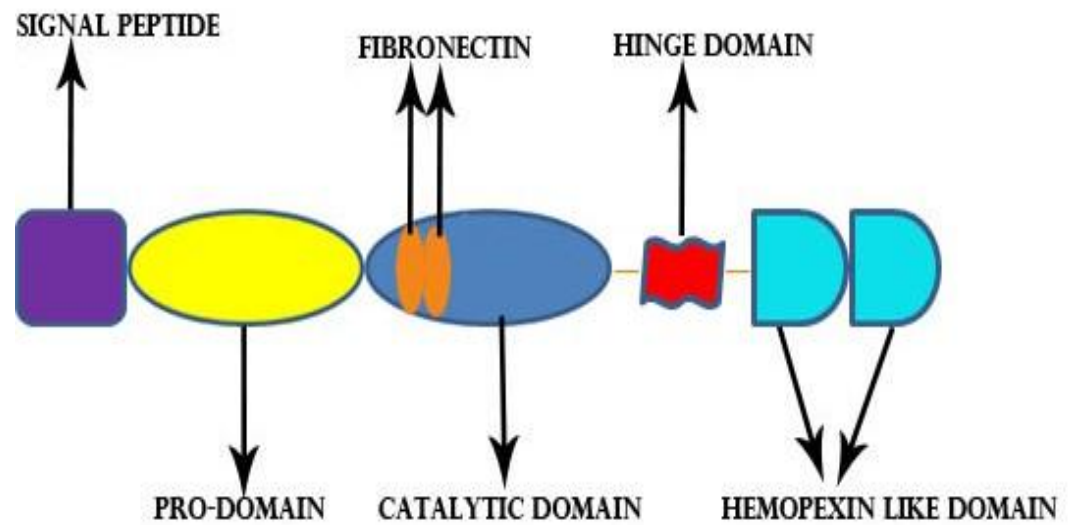


**Figure 2. Important Structural Features of MMP2** (Musheshe N, 2012)

## ***Drosophila Timp* (Tissue Inhibitor of Metallo-Proteases) Inhibits both *MMP1* and *MMP2***

TIMPs are tissue inhibitors of metalloproteases. They are endogenous protein inhibitors of MMPs and they occupy the active site of the enzyme. TIMPs also regulate the activity of some disintegrin and metalloprotease (ADAM) family proteases in mammals (Gomis-Ruth et al., 1997).

The *Drosophila* genome contains a single *Timp* gene. Deletion of fly *Timp* gives an inflated-wing phenotype, which could possibly result from loss of ECM that holds the two surfaces of the wing blade together (Godenschwege et al., 2000).

There are two-domain proteins of TIMPs. One protein has an N-terminal domain of about 125 residues in mammalian TIMPs. The N-terminal domain of TIMP can effectively inhibit a large number of MMPs (Brew et al., 2000).

The other domain protein is a smaller C-terminal domain of about 65 residues. Each domain contains three disulfide bonds that stabilize the structure (Brew et al. 2000).

In *Drosophila*, however, the N-terminal domain of TIMP lacks one disulfide bond that is conserved in other MMPs and therefore contains only two

of the three disulfide bonds found in the N-terminal domain of the recombinant protein in other MMPs.

Even though, the *Drosophila* TIMP inhibits both *Drosophila* MMPs (Page-McCaw et al. 2003), the N-terminal domain of TIMP inhibits MMP1 more effectively than it inhibits MMP2 (Wei et al., 2003). The N-terminal domain of TIMP inhibits ADAM proteases, a class of non-matrixin metzincin metalloproteases with a disintegrin-like domain (Stone et al. 1999).

*Drosophila* N-terminal domain of TIMP is very similar in structure to the mammalian N-terminal domain of TIMP-3. Both the *Drosophila* N-terminal domain of TIMP and the mammalian N-terminal domain of TIMP-3 have similar charge distribution on their surfaces which could explain why they can both inhibit the human necrosis factor-alpha-converting enzyme (TACE/ADAM17). *Drosophila* TIMP however, cannot inhibit ADAM10 (Wei et al., 2003)

## **Remodeling of the fat body**

The fat body serves as a food reserve of fatty tissue in the larval stages of certain insects such as *Drosophila melanogaster*. It is used as an energy source during hibernation and metamorphosis. Metamorphosis is characterized by

extensive tissue remodeling. The larval fat body is remodeled by undergoing tissue dissociation (Nelliot et al., 2006).

Fat body remodeling is the breakdown of a tissue made of closely associated and attached polygonal cells into individualized spherical cells. Tissue dissociation results in redistribution of individual fat cells throughout the body of the pupa.

If fat body remodeling is inhibited, however, lethality of the adult occurs and thereby associating fat body remodeling with completion of pupal development (Cherbas et al., 2003).

The detached fat cells in *Drosophila melanogaster* remain throughout metamorphosis, and are found in the newly eclosed adult as both free floating cells and as small clumps of cells.

It has been shown that the remodeling of the fat body also requires expression of *MMP2*. Because *MMP2* is attached to the membrane of cells by a GPI anchor (Page-McCaw et al., 2003), its localization supports the model for tissue-autonomous fat body remodeling.

Understanding the role of *MMP2* during tissue remodeling might enhance our understanding of cancer metastasis. The remodeling of the larval fat body takes place during early metamorphosis and is divided into three stages:

retraction, disaggregation, and detachment stages (Nelliot et al., 2006), as shown in Figure 3 below.

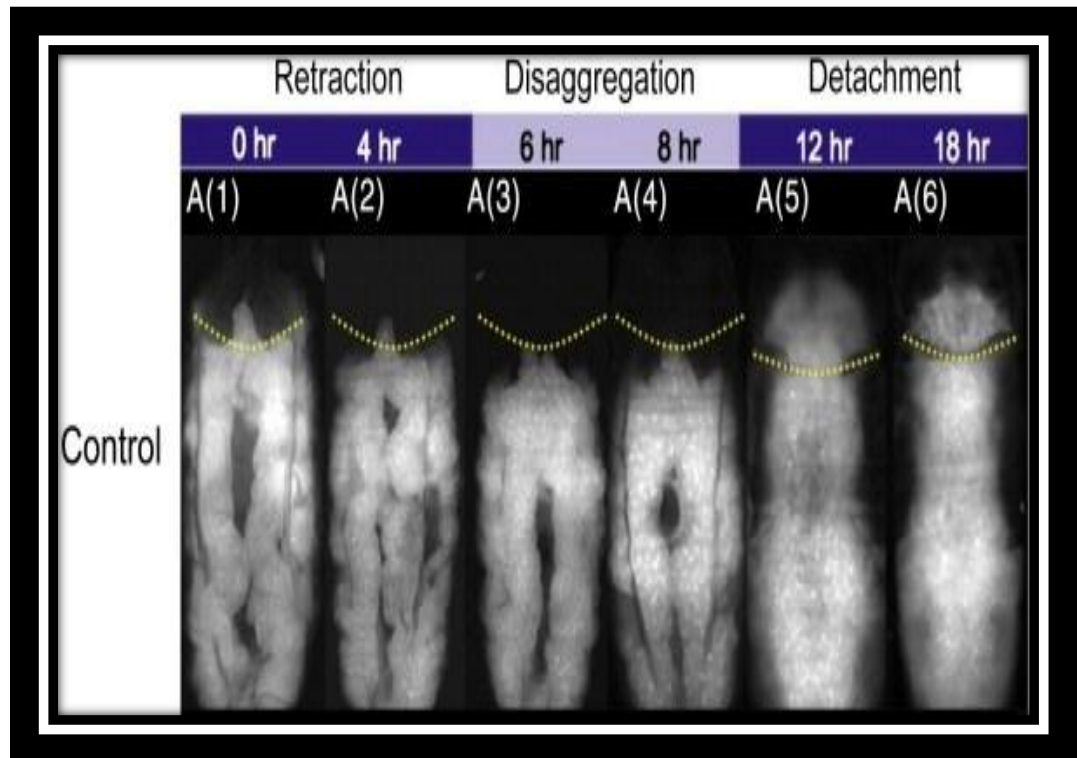


**Figure 3: Retraction, Disaggregation and Detachment Stages During Fat Body Remodeling in *Drosophila melanogaster*** (Bond N.D et al., 2011).

Retraction refers to the breaking away of the fat body from the walls of the 3<sup>rd</sup> larval instar as shown in Figure 3 (A1 and A2). During this stage, the cells shrink and move away from the animal's wall.

This is then followed by disaggregation, during which the cells begin to break apart as shown in Figure 3 (A3 and A4) and the individual cells become more visible.

The last stage of fat body remodeling is the detachment phase which involves the complete breakdown of the tissue of closely attached cells into single spherical cells as shown in Figure 3 (A5 and A6).

The single spherical cells move upwards into the head and to the rest of the animal body, and that is when head eversion occurs. The detachment phase of fat body remodeling occurs concurrently with expression of *MMP1* and *MMP2* during the prepupal to pupal transition stage (Nelliot et al., 2006; Page-McCaw et al., 2003).

Evidence has also shown that expression of *MMPs* might be regulated by *20-hydroxyecdysone* (20E) signaling making proteases candidates for involvement in fat body remodeling and possible target genes of the *βFTZ-F1*-mediated 20E signaling (Bond et al., 2011).

## **Steroid Hormones**

Steroid hormones trigger a wide variety of cell-specific responses such as programmed cell death during animal development (Baehrecke, 2000; Evans-Storm and Cidlowski, 1995). They are steroids that act as hormones. Because steroids are lipid soluble, they can diffuse easily through the cell membrane into



the cytoplasm of target cells and thereby induce a number of signaling cascades by binding nuclear receptors in the cell nucleus (Heffner and Schust, 2010).

Steroid hormones control metabolism, reproduction, and development in many organisms, and because of this, they have been linked to many human health problems. Steroids usually control major transitions in the life cycle, and they also regulate many distinct cell responses in a stage-specific way (Xiachun et al., 2012).

Steroid hormones may control salt and water balance, and in addition, the development of sex features. The mechanisms by which these signaling cascades specify cell division, differentiation, morphogenesis, or cell death are still unknown.

### **Steroid Hormones in *Drosophila***

There are three hormones that play a major role in the early life of *Drosophila*. These include: prothoracicotropic hormone (PTTH), juvenile hormone (JH), and ecdysone. PTTH initiates the synthesis and release of ecdysone from prothoracic glands and therefore PTTH may contribute to ecdysone titer changes that are important for development (Riddiford, 1993).

Juvenile hormone which is synthesized in the corpora allata is required at the time when ecdysone levels increase for larval molting. Juvenile hormone is also required to prevent metamorphosis. JH titer increases right before eclosion and it reaches its maximum titer level after eclosion (Riddiford, 2008).

Ecdysone is produced by the ring gland in *Drosophila melanogaster* in response to PTTH which is produced in neurosecretory cells (Riddiford, 1993). Ecdysone is not the active form of the hormone, but it is converted in the fat body and target tissues to 20-hydroxyecdysone (20E).

20E is the most active form of the ecdysteroids and it controls many aspects of *Drosophila* development. Ecdysone activates adult structure morphogenesis, as well as stage- and tissue-specific programmed cell death of the larval tissues.

There are two major ecdysone pulses that occur during each transition stage of metamorphosis. The first pulse occurs during embryogenesis and may play an important role in morphogenesis (Chavez et al., 2000). The first pulse triggers larval-prepupal transformation while the second pulse triggers the prepupal-pupal transition by means of a genetic regulatory pathway.

A combination of high levels of Juvenile Hormone and ecdysone pulses during the first two larval instars induces the two molts (Zhou and Riddiford., 2002). The first pulse during late third larval instar induces puparium formation, and thereby marks the beginning of prepupal development (Woodard et al., 1994).

The second pulse of ecdysone during which the levels of Juvenile Hormone have decreased occurs at about 10-12 hours after puparium formation (APF). This sharp increase in the ecdysone titer triggers head eversion, and therefore marks the prepupal-pupal transition of the larvae into pupa.

About 30hr After Puparium Formation, another large increase in 20E titer leads to adult development (Riddiford, 1993). The small amount of 20E that remains in the adult after eclosion quickly declines.

## **20E**

20E controls developmental processes in *Drosophila* through the heterodimeric receptor complex encoded by *Ecdysone Receptor (EcR)* and the *ultraspiracle (Usp)* genes (Koelle et al.1991, Thomas et al, 1993, Yao et al. 1992). The *EcR* produces three isoforms which can form heterodimers with *Usp* nuclear receptor family to form the receptor complex (Talbot et al., 1993).

The *EcR-Usp* complex in turn mediates specific developmental responses by binding to DNA elements located in the regulatory sequences of target genes in a stage-specific manner (Yao et al., 1992). The ecdysone receptor complex activates direct transcription of early genes. These early genes include; *Broad-*

*Complex (BR-C), E74A and E75* which in turn encode transcriptional regulators (Di Bello et al, 1991).

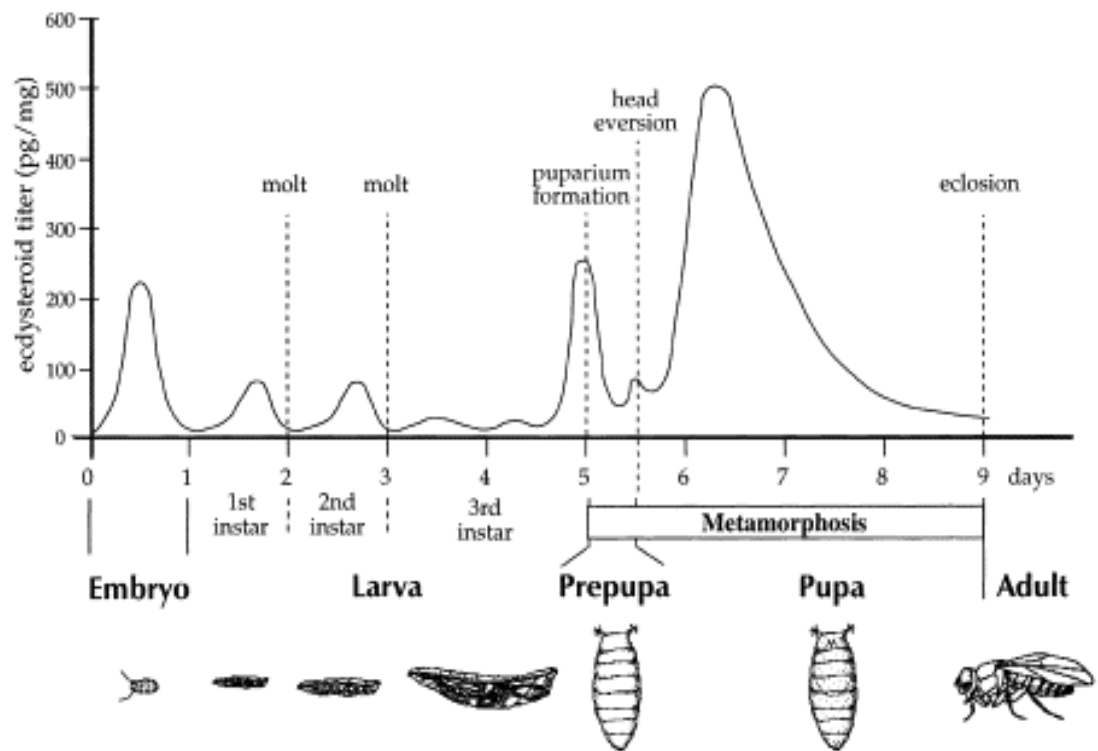


**Figure 4. Major Life Developmental Stages of *Drosophila melanogaster* Marked by Dots at Different Ecdysone Titer Levels (Riddiford, 1993).**

The end of each of the first two larval instars is marked by a molt as shown in Figure 4. The second pulse of ecdysone induces expression of the “early genes”- *Broad-Complex (BR-C)*, *E74A* and *E75* and in addition *E93* gene. An increase in 20E titer at the end of the third larval instar triggers puparium formation and marks the beginning of metamorphosis.

Shortly After Puparium Formation, the ecdysone titer decreases. 10-12 hours following puparium formation, the subsequent ecdysone pulse induces adult eversion (Lee and Baehrecke., 2001).

During metamorphosis of *Drosophila melanogaster*, successive pulses of the steroid hormone 20-hydroxyecdysone (20E) also lead to differentiation and morphogenesis of imaginal discs to give rise to adult tissues. They also trigger programmed cell death of larval cells to eliminate tissues such as the larval midgut, and anterior muscles (Thummel, C.S., 1996).

Other responses triggered by ecdysone during development in *Drosophila* include; remodeling of the central nervous system and deposition of pupal cuticle (Bender et al., 1997).

20E signaling is required within the fat body for the cell-shape changes and cell detachment that are characteristic of fat-body remodeling. The nuclear hormone receptor  $\beta$ FTZ-F1 is a key modulator of 20E hormonal induction of fat body remodeling and *matrix metalloproteinase 2* (*MMP2*) expression in the fat body. *MMP2* is necessary and sufficient to induce fat body remodeling and is a downstream target of the  *$\beta$ ftz-f1*-mediated 20E signaling cascade.

*$\beta$ ftz-f1* is a key regulator of tissue-autonomous fat body remodeling and is sufficient to induce fat-body remodeling in the presence of 20E signaling (Bond et al., 2011).  *$\beta$ ftz-f1* is expressed in the mid-prepupa between 6 and 10 hours APF when the 20E titer in the animal is low.

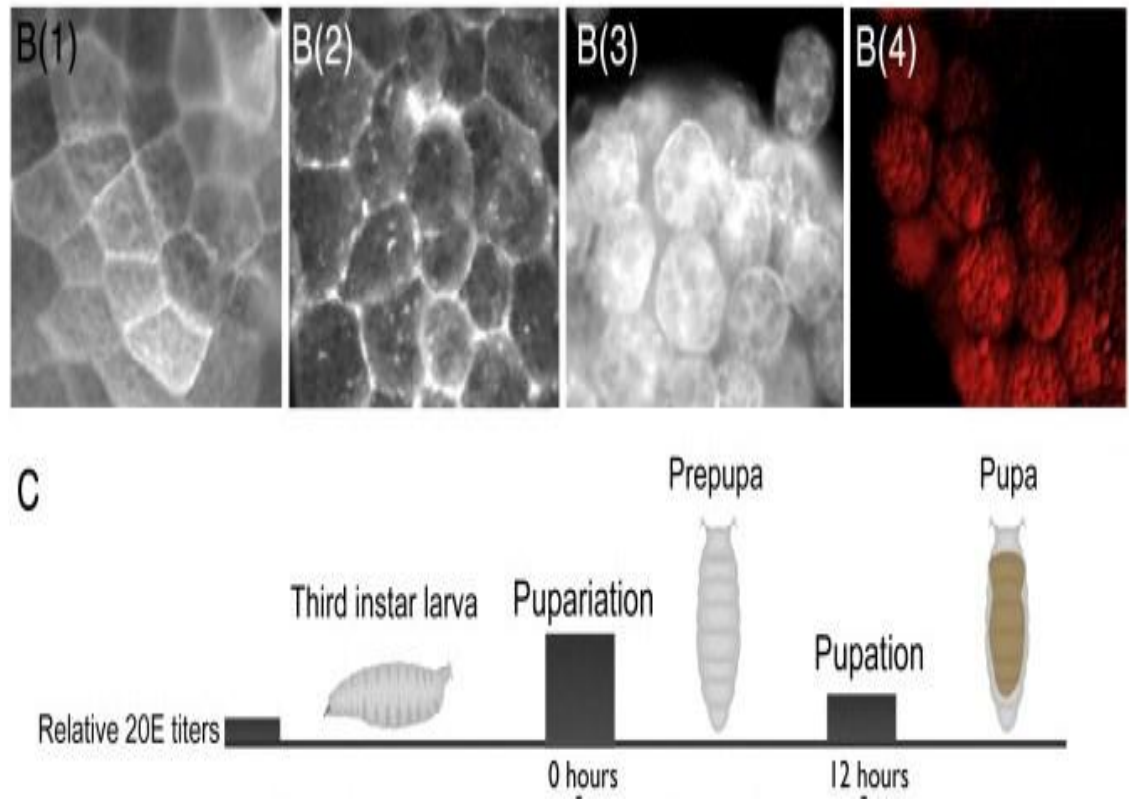


**Figure 5. Premature Expression of  $\beta ftz-f1$  During Fat Body Remodeling in *Drosophila melanogaster*** (Bond N.D et al., 2011).

Fat body remodeling in wild type *Drosophila* ( $w^{1118}$ ) does not begin to occur until after 12 hours APF. However premature expression of  $\beta ftz-f1$ , a nuclear receptor and key regulator of fat body remodeling before pupation as shown in Figure 5, triggers fat body remodeling (Bond N.D et al., 2011).

Figure 5 B(1) shows the fat body before remodeling occurs. Figure 5 B(2) shows cells of the fat body starting to break apart and the ECM lines around the cells becoming clearer.

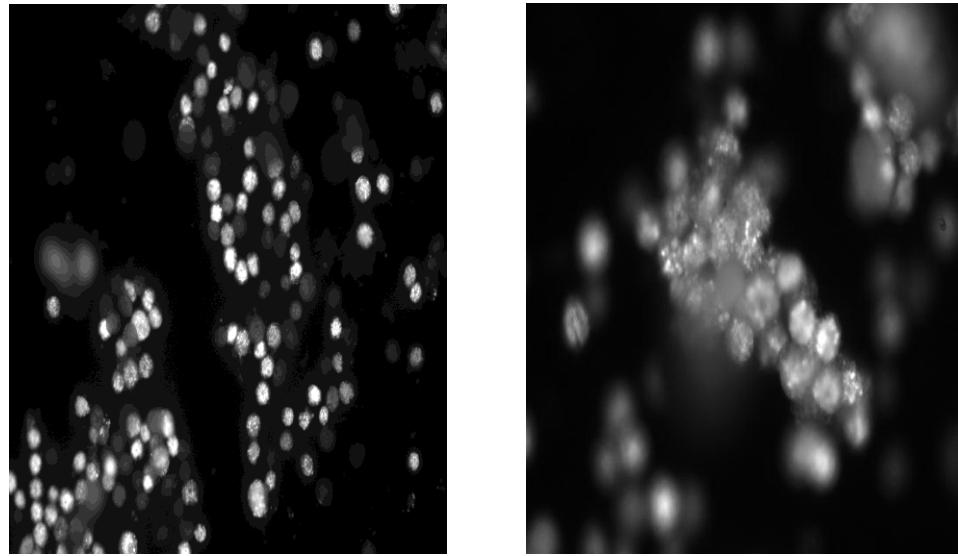
Figure 5 B(3) shows the cells in the prepupa disintegrating and the ECM breaking apart (Between 0 hours and 12 hours). Finally, Figure 5 B(4) at 12 hours shows the individualized spherical cells formed during pupation.

$\beta$ FTZ-F1, a nuclear receptor, is required for larval molting (Yamanda et al., 2000), and for the prepupal-pupal transition (Fortier et al., 2003). *βftz-f1* plays a role in the mediation of time-specific responses to changes in ecdysone titer.

It is also a competence factor for time and tissue specific responses to ecdysone (Broadus et al., 1999). *βftz-f1* also, activates transcription of the stage specific *E93* early gene (Woodard et al., 1994), which is specific to regulation of programmed cell death (Lee and Baehrecke., 2001).

## **E93**

In 2010, I discovered that *E93* is required for fat body remodeling by comparing wild type (*w<sup>1118</sup>*) and *E93* loss of function flies (*E93<sup>1</sup>/Df(3R)93F<sup>X2</sup>*), (work not yet published). By observing the fat body under the electronic microscope, it was noted that *E93* mutants had their fat body cells still clumped together at 13 hours APF while individualized single spherical cells were observed in the wild type flies as shown in figure 6.



**Individualized cells ( $w^{1118}$ )**

**Clumped cells ( $E93$  mutants)**

**Figure 6. Fat Body Remodeling in Wild type ( $w^{1118}$ ) and  $E93$  mutants** (Wai Yan Lam., 2012- unpublished).

$E93$  regulates many secondary response genes that function more directly in controlling developmental processes (Xiachun et al., 2012). 20E signaling is required for all expression of  $E93$  during metamorphosis. The steroid-regulated gene,  $E93$  plays an important role in larval salivary gland and midgut programmed cell death early in metamorphosis (Lee et al., 2000).

While a mutation in the  $E93$  gene prevents destruction of the larval salivary glands, only  $\beta ftz-f1$  is required for DNA fragmentation (Lee et al., 2002).  $E93$  mutants fail to undergo steroid-regulated programmed cell death.  $E93$  protein is bound to the sites of steroid-regulated genes and cell death genes on polytene



chromosomes and therefore *E93* mutants are defective in these genes (Lee et al., 2000).

The *E93* mRNA does not show any response to ecdysteroids in the late larval salivary glands, however, it is expressed 12 hours later in response to the prepupal ecdysteroid pulse. This in turn indicates that *E93* acts in a stage specific manner in response to the ecdysone titer. *βftz-f1* directs the stage specific induction of *E93* which leads to expression of *E93* at 12 hours APF.

During this same period, fat body remodeling occurs (Baehrecke and Thummel., 1995). *E93* is expressed in cells immediately before the onset of death (Lee et al., 2000), and this suggests that steroid stimulation of *E93* during development triggers a programmed cell death response.

## **Biochemistry of E93 protein**

*E93* is a 54 aa protein with a helix-turn-helix DNA binding domain of the Pipsqueak family (Siegmund and Lehmann., 2002). All *E93* orthologs contain nuclear receptor interaction motifs (LXXLL motifs), with an exception of one (Heery, D.M et al., 1997). *E93* contains three of the (LXXLL motifs).

This indicates that *E93* binds target enhancers together with the EcR or other nuclear receptors induced by ecdysone signaling (King-Jones, K and

Thummel, C.S., 2005). Additionally, all members of the E93 family contain an interaction motif (PXDSL/TXK/R) (Vo, N et al., 2001) for the co-repressor C-terminal binding protein (CtBP).

*E93* mutants are defective in preformation of the adult in metamorphosis. There are two complementation groups in the *E93* genomic region and these include; (93F) whose alleles cause lethality at the pupal stage, and *E93<sup>l</sup>* which contains alleles that cause death early in pupal development. *E93<sup>l</sup>* are defective in the death of larval salivary gland and midgut cells. The *E93<sup>l</sup>* allele has a nonsense change at codon 995 of the 1165 codon *E93* sequence (Xiachun, M et al., 2012).

Since *E93* is not expressed in the first 12hr of metamorphosis, shifts in target specificities occurring at the prepupal stage could be carried out by other factors that include ecdysone response genes. *E93* is expressed during the prepupal to pupal transition stage during which other genes that encode factors such as *MMP2* are also expressed. A figure showing expression of *MMP2* and *E93* during the second pulse of 20E is shown in Figure 7 below.

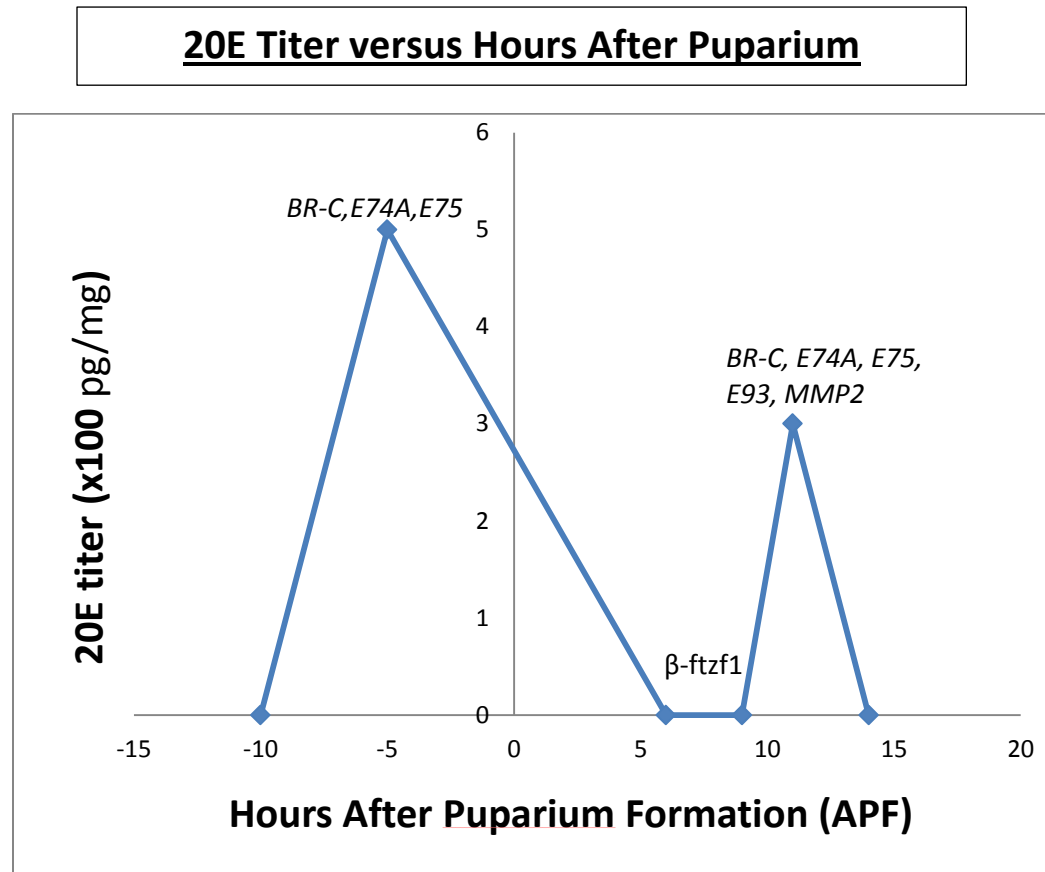


**Figure 7. Genes Expressed as a Response to 20E Signaling** (Bond et al., 2011). Figure 7 was generated in Microsoft Excel by Musheshe N., 2012.

The first pulse of 20E occurs between -4 and -8 hours After Puparium Formation. Between 6 and 10 hours After Puparium Formation, there are low levels of 20E, and there *βftz-f1* is expressed which is a competence factor for expression of other primary genes (*E74A*, *E75*, *BR-C* and in addition *E93*).

The second pulse of 20E during which *E93* and *MMP2* are expressed concurrently, occurs between 12 and 14 hours After Puparium Formation (Figure 7).

The goal of this project was to determine whether *E93* is required for the regulation of *MMP2* transcription levels during fat body remodeling in *Drosophila melanogaster*. *E93* loss of function mutants (*E93*<sup>1</sup>/*Df(3R)93F*<sup>X2</sup>) and wild type (*w*<sup>1118</sup>) were used to test for expression of *MMP2* in the fat body of both genotypes at 10 hours APF by using conventional Reverse Transcriptase PCR and Real Time quantitative PCR.

Since both *E93* and *MMP2* are thought to be required for fat body remodeling and they are both expressed during the same time of ecdysone pulse, I hypothesized that *E93* regulates expression of *MMP2* during fat body remodeling and therefore I predicted *E93* mutants would have low levels of *MMP2* expression.

## MATERIALS AND METHODS

### Stocks and Crosses

The mutant stock genotypes,  $E93^1/TM6B$  and  $Df(3R)93F^{X2}/TM6B$ , for this experiment were generously offered by Eric Baehrecke, Ph.D, School of Medicine, Cancer Biology and Graduate School of Biomedical Sciences, University of Massachusetts. The stocks were maintained on standard *Drosophila* media.

Control ( $w^{1118}$ ), and  $E93$  mutants ( $E93^1/TM6B$  and  $Df(3R)93F^{X2}/TM6B$ ) were kept under standard conditions at 25°C. In order to obtain virgin females,  $E93$  mutants were collected within 18 hours of eclosion at 18°C or within 8 hours of eclosion at 25°C. Reciprocal crosses of  $E93^1/TM6B \times Df(3R)93F^{X2}/TM6B$  were set up and then kept at 25°C to generate heterozygous  $E93^1/Df(3R)93F^{X2}$  flies. TM6B is the Third Multi-inversion balancer chromosome that was used in order to prevent crossing over between the homologous chromosomes during meiosis. Balancer chromosomes in general; suppress recombination with their homologs and they carry dominant markers thereby ensuring maintenance of heterozygous mutations.

Control (*w<sup>1118</sup>*) and *E93<sup>1</sup>/DF(3R)93F<sup>X2</sup>* mutant larvae were staged at puparium formation (the 0 hour prepupal stage), and placed on wet filter paper in Petri dishes at 25<sup>0</sup>C; they were kept in a non-air tight container for humidity and aged for 10 hours.

The fat bodies were dissected from 5 to 6 animals in a solution of 1x phosphate buffered saline (PBS) and then placed into a tube containing 30µl of PBS. 300µl of TriZol was then added to the tubes containing fat body and PBS. The fat body was crushed completely in order to homogenize the solution. The samples were then kept at -80<sup>0</sup>C until RNA isolation was done.

## **RNA Isolation**

The samples were transferred to a pre-centrifuged Phase lock Gel 2ml tube and they were spun at 12,000 rpm for 1 min. 60µl of chloroform were added to the samples and then the tubes were capped and shaken vigorously for 15 seconds by hand. Samples were then centrifuged at 12,000 rpm at 4<sup>0</sup>C. Chloroform denatures proteins and makes them soluble in organic phase or interphase and leaves nucleic acids in this case RNA in aqueous phase.

The clear aqueous phase formed on top of the Phase Lock Gel was transferred to a clean RNase-free tube. The phenol-chloroform and cloudy

solution was held below the Phase Lock Gel layer. 160µl of isopropanol were then added to the RNase-free tubes containing the clear aqueous phase. Isopropanol precipitates RNA, which forms a pellet during centrifugation. The solution was then shaken well and vortexed for better mixing. The samples were then precipitated overnight at -20<sup>0</sup>.

On the next day, samples were centrifuged at 14,000 rpm at 4<sup>0</sup>C for 20 minutes. The tube's hinge was aligned with the rotor as a way to easily identify the transparent flake-like pellet. The supernatant was carefully removed by pipet, and the pellet was washed with 500µl of 75% ethanol. The pellet was visible after addition of ethanol. The samples were then centrifuged at full speed for 5 minutes and the supernatant was then carefully removed.

Using a picofuge, the tubes were pulse centrifuged to collect all remaining ethanol at the bottom. The supernatant in each tube was removed by pipet and the pellet was allowed to air dry for 1 minute, which is just enough to make re-suspension easy.

The pellets in each tube were then redissolved in 5µl of RNase-free water to purify the RNA by eliminating RNases. The samples were then incubated at 60<sup>0</sup>C for 10 minutes to allow for dissolution. The sides of the tubes were flicked and vortexed a few times. The liquid in each tube was allowed to sit at room temperature for 5 minutes and finally frozen.

RNA concentration levels as well as protein concentration levels were then determined using the NanoDrop 3.1 spectrophotometer machine. 1 $\mu$ l samples of isolated RNA were tested. A good 260/280 absorbance ratio should be around 2. An absorbance ratio much lower than 2 indicates protein contamination. All the samples that were selected for cDNA synthesis had a 260/280 value above 1.9.

### **cDNA Synthesis**

The Invitrogen Superscript First-Strand Synthesis kit for RT-PCR with an Oligo(dT) primer was used to generate cDNA from the RNA templates. Master mix reactions were prepared for n+1 reactions.

Each component was centrifuged for a short time and then mixed before use. For the four RNA samples, a 0.5 ml tube was used to make a master mix of everything except the RNA. A master mix for 9 RNA reactions was made, as shown in Table 1.



**Table 1. Pipetting Scheme for One cDNA Synthesis Reaction**

Component	Amount for 1 Reaction
RNA	1 $\mu$ L
10mM dNTP mix	1 $\mu$ l
Primer (0.5 $\mu$ g/ $\mu$ l oligo (dt))	1 $\mu$ l
DEPC-treated water	7 $\mu$ l

The RNA/primer mixture was incubated in a heat bath at 65<sup>0</sup>C for 5 minutes after vortexing and then placed on ice for 1 minute. Both the oligo(dT) primers and random primers worked to build the cDNA template at the same time.

While Oligo(dT) primers add nucleotides to the leading mRNA strand's poly-A tail, random primers add six nucleotide fragments to the template. Another master mix was also prepared, as shown in Table 2.

**Table 2. Pipetting Scheme for the Second Master Mix for cDNA Synthesis**

Component	1 Reaction	10 Reactions
10X RT buffer	2 $\mu$ l	20 $\mu$ l
25mM MgCl <sub>2</sub>	4 $\mu$ l	40 $\mu$ l
0.1 M DTT	2 $\mu$ l	20 $\mu$ l
RNaseOUT (40 U/ $\mu$ l)	1 $\mu$ l	10 $\mu$ l

9  $\mu$ l of the master mix were added to the RNA/primer mixture formed previously and the mixture was collected by centrifugation after gentle mixing. The mixture was then incubated at 42<sup>0</sup>C for 2 minutes. 1  $\mu$ l of SuperScript<sup>TM</sup> II RT

was added to each tube except for the master mixes made for the control No-RT wells.

Instead, an extra 1 $\mu$ l of DEPC-treated water was added to the No-RT control reactions. All solutions were then incubated at 42 $^{\circ}$ C for 50 minutes. Following the incubation stage at 42 $^{\circ}$ C, the reverse transcriptase was inactivated by heating the reactions at 70 $^{\circ}$ C for 15 minutes.

The samples were collected by brief centrifugation, and 1 $\mu$ l of RNase H was added to each tube. They were then incubated at 37 $^{\circ}$ C for 20 minutes. cDNA samples were then stored at -20 $^{\circ}$ C.

## Primer Design

*MMP2* target gene Primers were synthesized by Integrated DNA Technologies (IDT) and designed from sequences provided by Flybase using the program on IDT website ([www.idtdna.com](http://www.idtdna.com)).

These primer sequences were:

*MMP2*

Forward: 5'-AGCAATCCGGAGTCTCGAGTCTTT-3'

Reverse: 5'-TGGAGCCGATTTTCGTGATACAGGT-3'

*Actin 5C* endogenous gene primers which produce an amplicon 158 base pairs long were used as a control on the cDNA samples. These were designed using NCBI Primer-Blast and FlyBase. They were synthesized by IDT too.

These primer sequences were:

*Actin 5C*

Forward: 5'-TCTACGAGGGTTATGCCCTT-3'

Reverse: 5'-GCACAGCTTCTCCTTGATGT-3'

Both the endogenous control and target gene primers were hydrated with nuclease-free water to obtain a diluted concentration of 10 $\mu$ M that was suitable for use in the Reverse Transcription Polymerase Chain Reaction.

## **Reverse Transcription Polymerase Chain Reaction (RT-PCR)**

RT-PCR was used to confirm the quality of cDNA samples and to ensure efficiency of the target gene primers. Two tubes for master mixes were prepared for *MMP2* and *Actin 5C* primers respectively. *Actin 5C*'s annealing temperature of 60.2<sup>0</sup>C was used in the RT-PCR. The *MMP2* primer set was used to confirm expression of *MMP2* in *w*<sup>1118</sup> and *E93*<sup>1</sup>/*DF(3R)93F*<sup>X2</sup> samples at 10hrs APF.

The annealing temperature for *MMP2* was determined by comparing brightness of the stained product and amount of product in No-RT samples.

Temperature for annealing *MMP2* primers was determined as 58.2<sup>0</sup>C (Bond et al., 2011).

n+1 reactions were prepared for RT-PCR using the pipetting scheme shown in table 3. 2 $\mu$ l of each cDNA sample and 48 $\mu$ l of master mix was added to make a total of 50 $\mu$ l in each tube (Table 3).

**Table 3. Preparation of Master Mix Reactions for RT-PCR**

Reagent	Amount added	Final concentration
10x PCR Buffer-MgCl <sub>2</sub>	5 $\mu$ l	1x
25mM MgCl <sub>2</sub>	6 $\mu$ l	3mM
10mM dNTPs	1 $\mu$ l	200 $\mu$ l
10 uM forward primer	2 $\mu$ l	400 $\mu$ l
10 uM reverse primer	2 $\mu$ l	-
cDNA	2 $\mu$ l	-
Water	31.6 $\mu$ l	-
Taq Polymerase	0.4 $\mu$ l	2 units
Final Volume	50 $\mu$ l	

Using a Tech Techgene thermocycler to amplify a precise region of DNA, each RT-PCR reaction was heated using the temperature profile shown in Table 4.

**Table 4. Temperature Profile for the Tech Techgene Thermocycler for RT-PCR**

Step	Temperature/ <sup>0</sup> C	Time/s	Cycle count
Separation	94	30	35 cycles
Annealing	Varied	30	35 cycles
Extension	72	30	35 cycles
Final extension	72	300	1 cycle
Final hold	4	-	-

The separation stage involves melting of double stranded DNA template by breaking down hydrogen bonds. During annealing stage, the forward and reverse primers bind to the newly single-stranded template.

The extension stage following the annealing stage involves synthesis of a complementary DNA strand by DNA polymerase. At 100% efficiency, DNA target is doubled at each elongation stage. This results in exponential amplification of DNA.

## **Gel Electrophoresis**

Agarose gel electrophoresis was used to analyze conventional RT-PCR products. 0.8 g of agarose, 50 mL of tris-acetate EDTA (TAE) buffer, and 5 $\mu$ l of 10  $\mu$ g/mL ethidium bromide (EtBr) were mixed to form a 1.6% agarose gel. EtBr is a fluorescent molecule that binds to double-stranded DNA.

EtBr allows for visualization of DNA bands under UV light. The prepared agarose gel was allowed to polymerize for about 20 minutes before loading samples. It was then submerged in 1X TAE buffer. 100 base pair ladder was loaded into well 1.

The base pair ladder can be used to measure the size of the bands. 20 $\mu$ l of each sample were loaded into wells 2-9. No-RT controls and RT containing genes were all loaded. The gel was run for 1 hour and 20 minutes at 150V. The image was taken using the Fujifilm LAS-3000 with ImageReader LAS-3000 software.

Primer amplification of the target genes was confirmed by observing the position of DNA bands in the wells and comparing their sizes to those of the base pair ladder. DNase treatment is usually performed before Gel Electrophoresis to get rid of genomic DNA.

## **Primer Optimization**

Because conventional RT-PCR plus gel electrophoresis are not sufficient and accurate for quantifying PCR products, quantitative Real Time PCR (qPCR) was therefore employed to quantify accumulation of PCR products in each amplification cycle.

Primer optimization greatly increases probability of amplification of target DNA by eliminating primer dimers and thus providing more primers for annealing to the target.

There are two methods that can be employed in order to detect accumulation of PCR products. These include; 1) use of SYBR Green, a fluorescent dye that only binds double stranded DNA and 2) use of a custom-designed TaqMan probe which when combined with an amplicon releases a fluorophore. Even though use of a TaqMan probe is expensive, it allows for amplification of multiple target genes in one reaction.

qPCR for optimizing primer concentrations was performed using PerfecCta<sup>TM</sup> SYBR<sup>®</sup> Green Supermix, ROX (Quanta Biosciences) on an ABI 7300 Real Time PCR machine. In this technique, care was taken to design primers that will not amplify primer dimers. This is because SYBR green binds any double stranded DNA present in the sample and thereby resulting in less accurate results.

The cDNA used in the qPCR assay was single stranded since the RNA template had been destroyed by the RNase H treatment. Therefore as the qPCR proceeds, the SYBR Green binds to the dsDNA that accumulates.

cDNA concentration levels were determined using the NanoDrop 3.1 spectrophotometer machine. 1µl samples of cDNA were tested. All the samples

that were selected for qPCR had a 260/280 value above 2.0. Series dilutions of  $w^{1118}$  cDNA were then made with a starting concentration of 260ng.

Samples included; 26ng, 2.6ng, 0.26ng and 0.026ng. Two master mixes were prepared, one containing *MMP2* and another containing *Actin 5C* forward and reverse primers respectively. A pipetting scheme for qPCR is shown in Table 5.

**Table 5: Pipetting Scheme for qPCR**

Reagent	Amount added	Final concentration
2x Perfecta SYBR Green, Super mix with ROX	11.25 $\mu$ l	1x
Forward Primer	2.5 $\mu$ l	100-500nm
Reverse Primer	2.5 $\mu$ l	100-500nm
RNase free water	6.25 $\mu$ l	
cDNA	2.5 $\mu$ l	
Final Volume	25 $\mu$ l	

To 17.5 $\mu$ l of the master mix, 2.5 $\mu$ l of the forward and 2.5 $\mu$ l of the reverse primers at the appropriate concentration were added to each well, and mixed thoroughly in the 96-well plate (layout of 96-well plate is shown in Table 11).



To this 22.5 $\mu$ l mixture, 2.5 $\mu$ l of each respective cDNA concentration was added to each well. No-RT samples were also run on the plate as a way of evaluating primer dimer formation. After loading all the samples, the plate was sealed with a plastic cover. The samples were tapped gently to allow for mixing.

The plate was then placed into the ABI 7300 machine and the qPCR cycle was run as shown in Table 6 (Plate set-up is shown in the appendix-Table 11). The experiment took about 3 and half hours.

**Table 6: Cycles of qPCR**

Stage of cycle	Temperature/ $^{\circ}$ C	Time	Reps	Step	Action
Stage 1	90	2 mins	1		
Stage 2	95 55 72	15 secs 1 min 1 min	40	Denaturation  Extension	Data Collection
Stage 3	95 60 95	15 secs 1 min 15 secs	1		Dissociation step

The dissociation step is added at the end of stage 3 as a way of ensuring dissociation of primer dimers that SYBR Green would otherwise bind to because they are also double stranded.

The cycle number at which the target DNA is amplified exponentially is known as the Cycle threshold,  $C_t$ . At the  $C_t$  value, the level of fluorescence in that cycle exceeds that of the background. Cycle threshold ( $C_t$ ) values and melting curves for each primer concentration pair were used to determine optimum primer concentrations.

Therefore a low  $C_t$  value indicates a higher concentration of mRNA from the gene of interest that is amplified and thereby allowing for earlier fluorescence. A low  $C_t$  value also indicates that the reaction has reached the exponential amplification phase earlier (Figure 12 and 13 shown in the appendix). When the mRNA of the gene does not exceed a certain threshold, then the matching  $C_t$  value is undetermined. Primer pairs with the lowest  $C_t$  values were chosen.

Melting and dissociation curves were also generated by the ABI 7300 software qPCR machine and they were used to separate the unified double stranded DNA that had been amplified. The two DNA strands are separated at the melting point thereby decreasing fluorescence fast.

The single large peak formed on the “rate of change of fluorescence vs. temperature” plot indicated amplification of the single cDNA target gene. The melting temperature at which the peak is formed is the temperature at which the double stranded cDNA is reduced to the single stranded cDNA. A sample dissociation and melting curve is shown in Figure 8.

### Rate of Change of Fluorescence versus Temperature

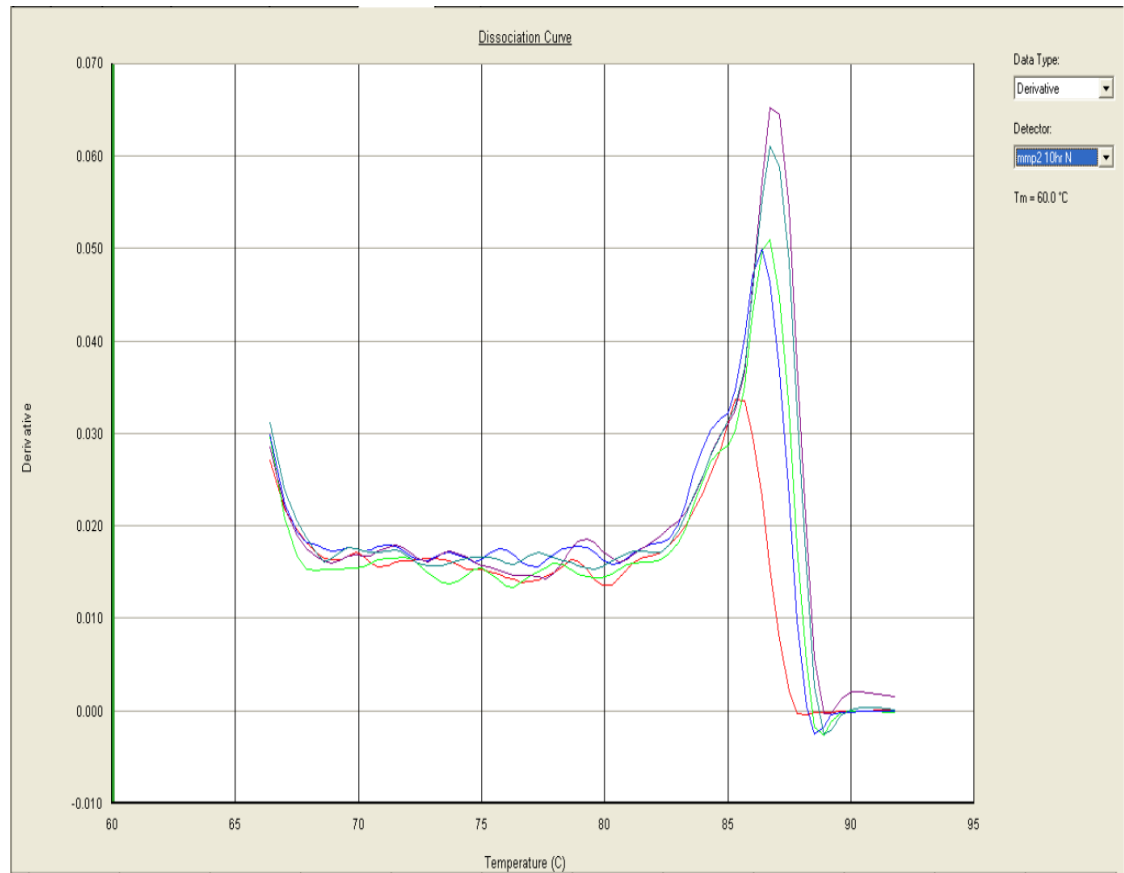


**Figure 8. Dissociation Curve for *MMP2* using 500nm Forward Primer: 500nm Reverse Primer set.**

Figure 8 shows a plot of the derivative of fluorescence intensity as a function of temperature in degrees Celsius. The peaks show respective wells in which a single target cDNA had been amplified.

## Calculation of Primer Efficiency

After qPCR optimization of primers, primer efficiency was tested. 100% efficiency occurs when the quantity of DNA doubles with every cycle during the linear phase of amplification. If the primers produce more than double the DNA in every cycle, they are referred to as over efficient (>100%). On the other hand, if they produce less than double the amount of DNA in each cycle, they are referred to as under efficient (<100%). Standard curves of the target genes were generated in order to determine primer efficiency.

The numerical  $C_t$  values determined using 7300 BioAnalyzer software were exported to Microsoft Excel to generate primer efficiency calculation graphs. Plots of  $C_t$  values vs. log cDNA concentration were made to obtain the slope. A slope of -3.32 indicates 100% efficiency of primers, a slope above -3.32 indicates over efficiency while that below -3.32 represents under efficiency of primers. Primer efficiency was calculated using the equation shown below:

$$\text{Efficiency} = [10^{-1/\text{slope}}]$$

A sample standard curve generated using Microsoft Excel is shown in figure 9. Efficiency close to 2 indicates efficient primers. Efficiency below 2 indicates under efficiency of primers, while efficiency above 2 indicates over efficiency of primers.

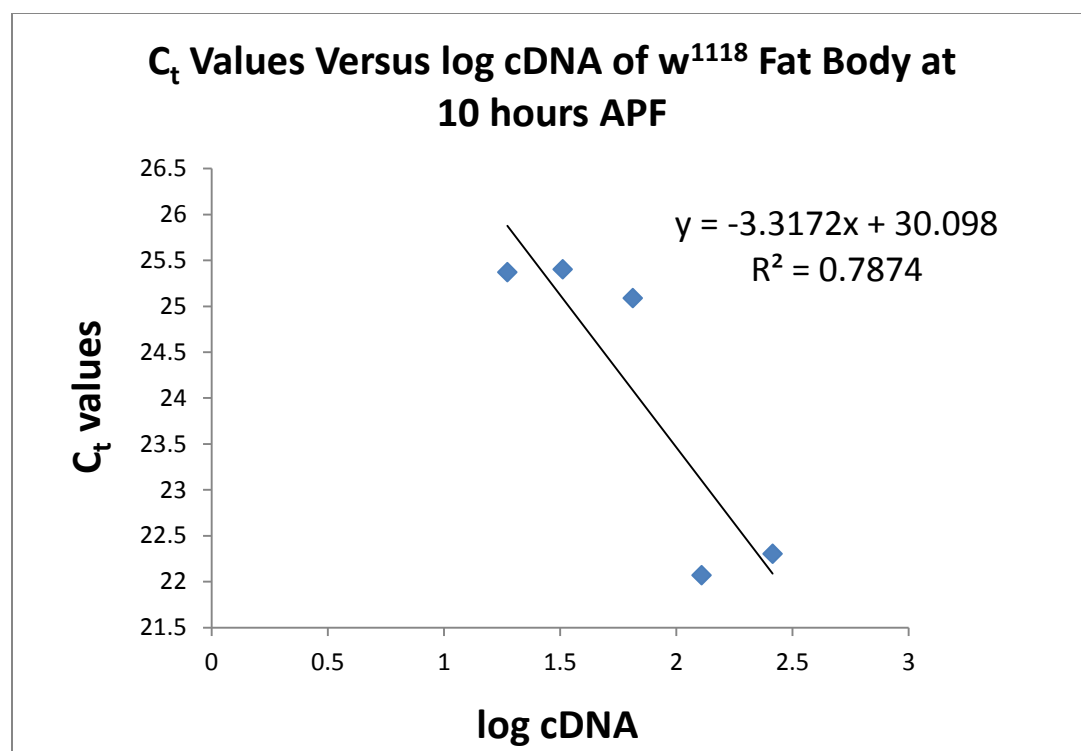


**Figure 9. Standard Curve Generated to Calculate Primer Efficiency of *MMP2* Primers at 10hrs APF of control (w1118) cDNA.**

In figure 9, the x-axis is the log of cDNA of each serial dilution (undiluted, 1/2, 1/4, 1/8, and 1/16). The y-axis includes the threshold C<sub>t</sub> values that were obtained from the ABI 7300 BioAnalyzer software report.

Primer efficiency calculated from the graph with equation,  $y = -3.3172x + 30.098$  and  $R^2 = 0.7874$  above, is 100.2% efficient or 2.002. This indicates that the target primers (*MMP2*) were efficient. The *MMP2* primers were optimized to 500nm forward and 500nm reverse, while the *Actin 5C* were optimized to 300nm forward and 100nm reverse (Bond et al., 2011).

Primer efficiencies of the house keeping gene (*Actin 5C*) and gene of interest (*MMP2*) were compared in order to decide an appropriate quantification method. There are two quantification methods and these include;  $\Delta\Delta C_t$  quantification and standard curve quantification methods.

The  $\Delta\Delta C_t$  method is used if the primer efficiencies of the house keeping gene and gene of interest are between 90% and 110% and with not more than 5% difference with each other. In case the primer efficiencies for the house keeping gene and target gene differ by more than 5%, and are each way out of the range of acceptable primer efficiency values, then standard curves are made for each plate to ensure accuracy.

Also, standard curves are made for each plate to ensure that the best primer sets are used for experimental qPCR in order to determine target gene expression levels in the mutants.

## **Experimental qPCR**

After optimizing the primers and calculating the primer efficiency for both the endogenous and target genes, an experiment for four reactions at 10 hours APF fat body was carried out:  $w^{1118}$  with *Actin 5C* primers,  $w^{1118}$  with *MMP2*

primers,  $E93^1/Df(3R)93F^{X2}$  with *Actin 5C* primers and  $E93^1/Df(3R)93F^{X2}$  with *MMP2* primers (plate set-up is shown in Table 13-appendix).

Each set of the reactions was run on the 96-well plate in triplicate i.e. No-RT controls were included. Master mixes for n+2 reactions were prepared using a procedure shown in Table 5. The qPCR experiment was run using the 7300 BioAnalyzer software to generate expression data for the target gene (*MMP2*) in the mutants ( $E93^1/Df(3R)93F^{X2}$ ).

### **Calculation of fold change in qPCR**

Fold change is used in analysis of gene expression. It defines how much a quantity being measured changes as it goes from an initial to a final amount. Because of technical variability among experiments, the  $C_t$  values of the target gene (*MMP2*) were normalized to the  $C_t$  values of the endogenous gene (*Actin 5C*) in order to give a normalized differential expression,  $\Delta C_t$ .

Average  $C_t$  values were calculated for each set of samples and the differential expression for measuring the expression of the target gene (*MMP2*) was calculated for both the control and experimental samples. Equations used are shown below;

$$\Delta C_{tControl} = C_{tTarget} - C_{tEndogenous}$$

$$\Delta C_{tExperimental} = C_{tTarget} - C_{tEndogenous}$$

Since in every cycle in PCR, the amount of DNA is approximately doubled, the  $C_t$  is in a logarithmic phase and inversely proportional to the amount of the quantity of DNA/RNA. This means that high  $\Delta C_t$  values represent low expression while low  $\Delta C_t$  values indicates high expression of genes (Ramon et al., 2009).

The normalized differential expressions are not enough to compare the experimental results to the control genotype and therefore they were subtracted to reflect the difference between the experimental treatment and control to obtain  $\Delta\Delta C_t$ . Equation that was used is shown below;

$$\Delta\Delta C_t = \Delta C_{tExperimental} - \Delta C_{tControl}$$

From  $\Delta\Delta C_t$ , the fold change was calculated to determine whether the target gene had been down regulated in the mutants. The fold change is an expression ratio; if the fold change is positive, then the target gene has been up-regulated. But if the fold change is negative, then the target gene has been down regulated (Livak and Schmittgen, 2001).

Fold change in the experimental treatment can be obtained utilizing the equation shown below;

$$\text{Ratio} = [(E_{\text{target}})^{\Delta C_{tTarget}}] / [(E_{\text{reference}})^{\Delta C_{tReference}}]$$



A value of less than one indicates under expression in the experimental sample while a value greater than one indicates over expression of the target gene.

## RESULTS

### Confirmation of the role of *E93* in fat body remodeling

The role of *E93* during fat body remodeling was confirmed during dissection of *E93* loss of function fat body and control fat body at 13 hours APF. It was evident under the electronic microscope that the salivary glands had not been destroyed in the mutants, and the fat body had also not undergone complete remodeling. The cells in *E93* mutants fat body were still clamped together as opposed to the individualized spherical cells as observed in the control.

### Confirmation of *MMP2* expression using RT-PCR

Expression of *MMP2* in fat body cDNA of the control (*w<sup>1118</sup>*) and *E93<sup>1</sup>/Df(3R)93F<sup>X2</sup>* at 10 hours APF was confirmed using RT-PCR. The samples of cDNA were run on a 1.6% Ethidium Bromide stained Agarose gel to observe the quality of the bands formed against a 100 bp ladder.

*Actin 5C* was used as the housekeeping gene and No-RT samples were also run for each primer set for both the control ( $w^{1118}$ ) and  $E93^1/Df(3R)93F^{X2}$  as shown in Figure 10.

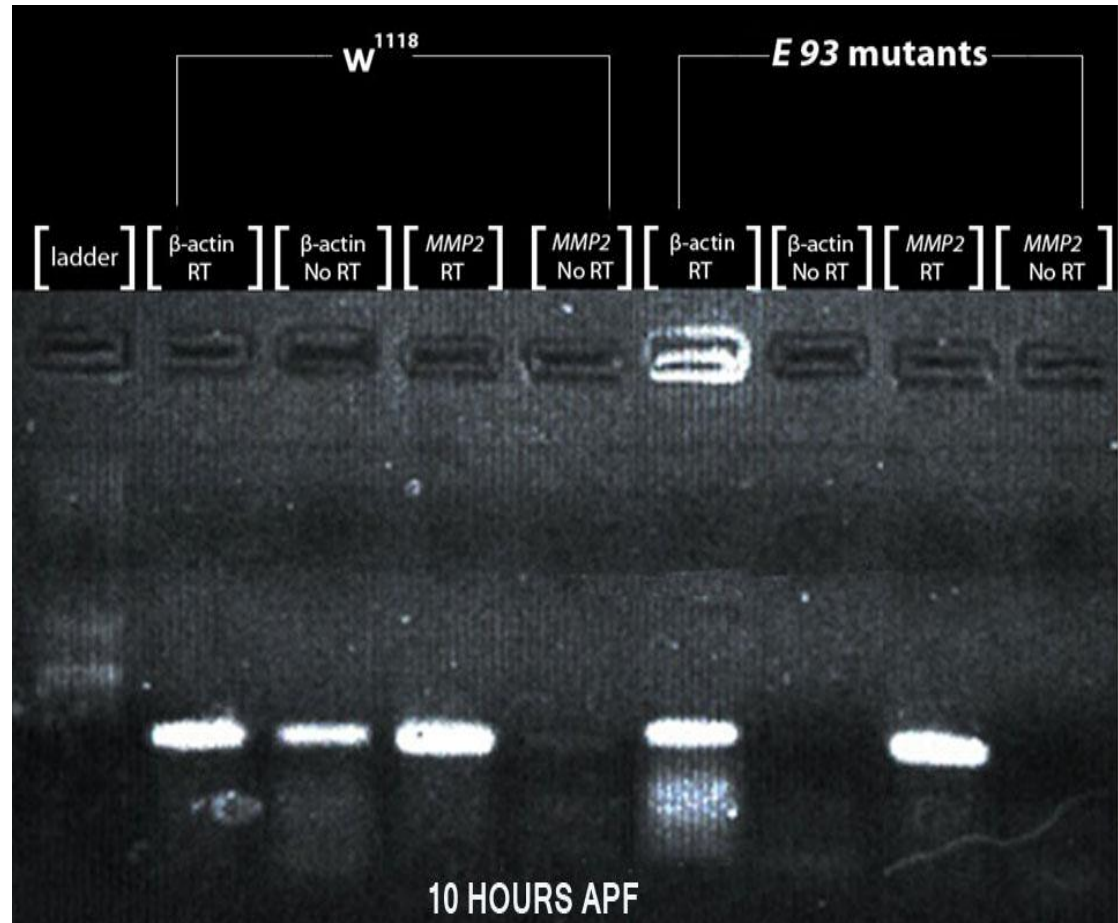


**Figure 10. 1.6% Ethidium Bromide-Stained Agarose Gel.**

Fat body cDNA samples from  $w^{1118}$  and  $E93^1/Df(3R)93F^{X2}$  were tested using RT-PCR. The bright and thick bands are of amplified cDNA. Even though there was a band in the *Actin 5C* well with No-RT that could have been genomic

DNA, experiments were still carried on since it had minimal effect on the composition of the other samples.

The extra bands observed are of primer dimers. Overall, the presence of cDNA indicates that *MMP2* is expressed in *Drosophila melanogaster* at 10 hours APF.

### **Primer efficiencies in qPCR**

Using 7300 BioAnalyzer software, amplification plots for the target gene and endogenous gene were generated using annealing temperatures shown in Table 7. Five different concentrations with the appropriate primer concentrations were run in a 96-well plate to obtain amplification and dissociation plots (plate set-up is shown in Table 12-appendix).

**Table 7. Annealing Temperatures for *MMP2* and *Actin 5C* Primers used in the Instrument Set-up**

Primer	Annealing temperature
MMP2	58.2 <sup>0</sup> C
<i>Actin 5C</i>	58.2 <sup>0</sup> C

Annealing temperature for *MMP2* primers was used to run the experiment, and therefore the annealing temperature of *Actin 5C* was lower than its optimum temperature of 60.2<sup>0</sup>C. Primer set concentrations used for both the endogenous and target genes are shown in Table 8.

**Table 8. Primer set concentrations for endogenous gene and target genes used.**

Primer set	Primer set concentration ratio
<i>Actin 5C</i>	300:100 (forward:reverse)
<i>MMP2</i>	500:500 (forward:reverse)

C<sub>t</sub> values were obtained from the 7300 BioAnalyzer report and they were exported to Microsoft Excel in order to generate standard curves from which the slopes were obtained to calculate primer efficiencies shown in Table 9.

**Table 9. Primer Efficiencies Obtained from Standard Curves**

Primer Set	Slope	Efficiency
<i>MMP2</i>	-5.8206	1.724
<i>Actin 5C</i>	-7.9267	1.262

The primer efficiencies were both below 2 but quite close in range and therefore they were still used to determine expression levels of the gene of interest (*MMP2*).  $\Delta C_t$  values are shown in Table 10 below.

**Table 10.  $\Delta C_t$  values of the control ( $w^{1118}$ ) and  $E93^1/Df(3R)93FX2$  obtained from Experimental qPCR.**

Genotype with primer set	$\Delta C_t$
$w^{1118}$ <i>MMP2</i>	14.17
$w^{1118}$ <i>Actin 5C</i>	21.95
$E93^1$ <i>MMP2</i>	21.53
$E93^1$ <i>Actin 5C</i>	33.07

$$\Delta C_{t \text{ Control}} = 14.17 - 21.95$$

$$= -7.78$$

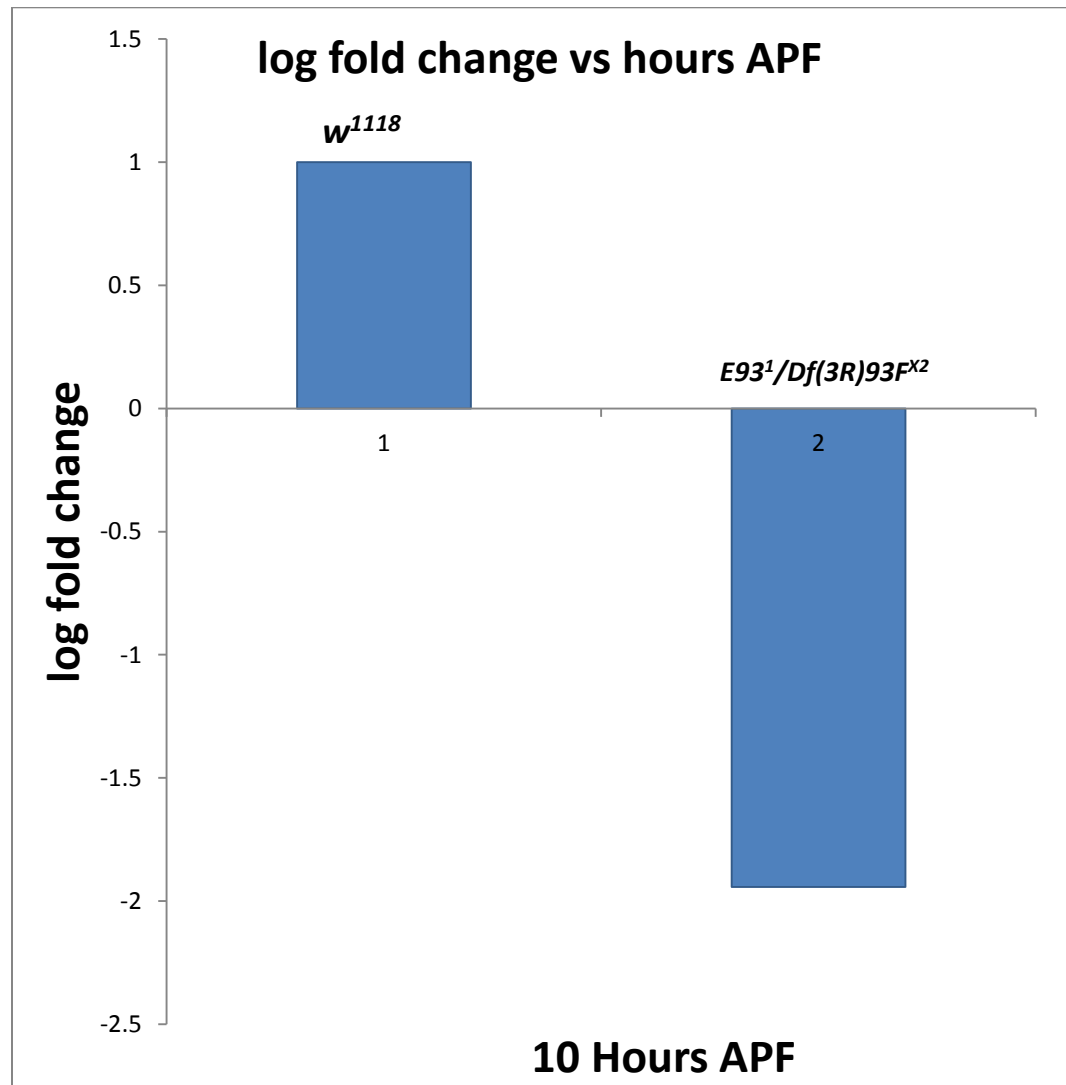
$$\Delta C_{t \text{ Experimental}} = 21.53 - 33.07$$

$$= -11.54$$

$$\text{Ratio} = (E_{\text{target}})^{\Delta C_{t \text{ Target}}} / (E_{\text{reference}})^{\Delta C_{t \text{ Reference}}}$$

$$= (1.724)^{-11.54} / (1.262)^{-7.78}$$

$$= 0.011392$$

**Expression of *MMP2* in *E93<sup>1</sup>/Df(3R)93F<sup>X2</sup>* at 10 hours APF**

**Figure 11. Relative Expression of *MMP2* in *E93<sup>1</sup>/Df(3R)93F<sup>X2</sup>* (Musheshe N, 2012)**

A value of fold change above 1 indicates over expression of target gene, while that below 1 indicates under expression of the target gene. From Figure 11 above, Wild type fold change is at the maximum of one, while that of the *E93* mutants is less than 1. Since the value obtained for the *E93* mutants, 0.011392, is less than one, then expression of *MMP2* was downregulated in *E93<sup>1</sup>/Df(3R)93F<sup>x2</sup>* at 10 hours after puparium formation. In other words, the bar chart confirms relative expression of *MMP2* as downregulated since the bar is below positive 1.

These results are however, not so conclusive since they were calculated using under efficient primers.



## DISCUSSION

### **Expression of *MMP2* in the Fat Body of *w<sup>1118</sup>* and *E93<sup>1</sup>/Df(3R)93F<sup>X2</sup>* at 10 hours APF**

Downregulation of *MMP2* occurred in *E93<sup>1</sup>/Df(3R)93F<sup>X2</sup>* samples which suggests that transcription of *MMP2* may be regulated by *E93*. Current studies have shown that *MMP2* is required for fat body remodeling. The pre-mature expression of *MMP2* results in fat body remodeling (Bond et al., 2011).

It has been shown that fat body remodeling does not occur if EcR-DN, a negative ecdysone receptor is present in the animal. This indicates that fat body remodeling requires ecdysone signaling in order to occur. *MMP2* is expressed during periods of high ecdysone titer which shows that *MMP2* expression requires an increase in the levels of ecdysone.

However, if *MMP2* expression was only dependent on ecdysone, then fat body remodeling would have occurred earlier in the life time of *Drosophila melanogaster*, most probably at the time of high ecdysone titer which leads to pupariation but it does not.

The results obtained, suggest that a mutation in *E93*, leads to a decrease in expression of *MMP2*. This suggests therefore that *E93* may be a positive regulator of *MMP2*.

By prematurely expressing *Bftz-f1* in the fat body, *MMP2* is found to be upregulated and thereby suggesting a role of *Bftz-f1* in *MMP2* regulation (Bond et al., 2011). BFTZ-F1 protein is present at the time of expression of *MMP2* suggesting either a direct or indirect role of *Bftz-f1* in *MMP2* expression (Yamanda et al., 2000).

Since *Bftz-f1* has also been shown to regulate *E93* expression in other larval tissues such as the salivary glands (Bond et al., 2011), my results which show downregulation of *MMP2* expression in the absence of *E93*, may suggest an indirect role of *Bftz-f1* in *MMP2* expression.

These results suggest that *Bftz-f1* may act directly on *E93* to turn on *E93* expression, and in turn *E93* may act directly to turn on *MMP2*.

## **Implications of Downregulation and Upregulation of *MMP2***

The fat body is a nutritional reserve as well as an essential organ for fueling metamorphosis. If it fails to undergo complete remodeling, then normal

development processes of *Drosophila melanogaster* will be prevented and the consequences may be fatal. Both *E93* and *MMP2* are required for fat remodeling.

*MMP2* is expressed concurrently with detachment phase, which is the last stage of fat remodeling. In the event of low levels of *MMP2* which is responsible for degrading the Extra Cellular Matrix as well other complex proteins, the cells are unable to break apart into individualized spherical cells, thereby inhibiting migration of the cells.

Although this could be necessary to prevent invasion of tissues in the event of disease development in humans, it also poses disadvantages that include: limited intercellular communication which is required for the onset of immune responses i.e. inflammatory responses during infection by microorganisms, and also may lead to disrupted insulin signaling.

In *Drosophila*, low levels of *MMP2* may lead to failure of completion of fat body remodeling and therefore head eversion may not occur thereby leading to incomplete metamorphosis, and failure of puparium formation. Lethality may also occur among the mutants.

In the event of upregulation of *MMP2*, *MMP2* may over degrade the ECM leading to an increased loss of cells as well as increased damage to the basement membrane of the tissue. In humans, upregulation of *MMP2* may lead to an excessive breakdown of laminin-5 and collagen IV of the ECM, resulting in increased space for facilitating tumor growth.

In addition, upregulation of *MMP2* in *Drosophila* may provide evidence on the role of MMPs in cancer metastasis and whether invasive tumor progression in humans would increase with increase in *MMP2* levels.

### **Future studies of MMPs and E93 in *Drosophila***

Since the primer efficiencies for the housing keeping gene and target gene in the experiments differed by more than 5%, and were each way out of the range of acceptable primer efficiency values, then standard curves will be made for each plate to ensure accuracy.

### **Transmission Electron Microscopy**

This will be used to observe the fat body of both the control ( $w^{1118}$ ) and mutants ( $E93^1/Df(3R)93F^{X2}$ ) to see if there will be no detachment phase of fat remodeling and therefore the cells will appear distinct from one another but they will still be attached. Also, no or very few individualized spherical cells will be distributed throughout the body of the animal.

By using the *Drosophila melanogaster* model to examine the role of MMPs in tissue remodeling, a better understanding of how MMPs play a role in signaling pathways, such as insulin signaling, will be achieved. Since the role of MMPs in normal development processes is still unclear, the use of a *Drosophila* model presents an opportunity for our insight on the roles of the metalloproteinases whose roles are poorly understood in humans.

A mutation in *E93* may reveal more information about the role of *E93* in programmed cell death and fat body remodeling. *E93* is expressed at the time of programmed cell death of some larval tissues, such as the salivary gland, but also during fat body remodeling.

The mechanisms by which the gene participates in either programmed cell death or fat body remodeling during development of *Drosophila melanogaster* are still unknown. However, by studying more about the regulatory functions of *E93* of other genes, a better understanding of its exact role in programmed cell death will be obtained.

The study of MMPs and regulation of their transcription is very crucial because MMPs such as *MMP2s* are found to be elevated in cancer in humans. The breakdown of the Extra Cellular Matrix involves increase in mobility of cells and therefore poses a benefit for cancer metastasis.

Therefore studies using the *Drosophila* model on how *MMP2* transcription could be switched on or off may bring research closer to a solution aimed at

preventing rapid cancer metastasis, and also increase our understanding on the role of the proteins-MMPs in normal development processes and as well disease processes that we are otherwise unable to study in humans due to their redundant nature (Page-McCaw et al., 2007).

## **SOURCES OF ERROR IN THE EXPERIMENT**

Pipetting errors may have occurred during preparation of the 96-well plate of the Experimental qPCR since it was larger and required speed to fill up to prevent the plate from drying up.

Some of the SYBR green could have fluoresced during preparation of the plate due to sunlight/light bulb exposure. Mainly, errors could have occurred during either one of the procedures involved in qPCR i.e. from RNA isolation to finding concentrations using the NanoDrop machine and finally to preparing the 96-well plate for qPCR.

## APPENDIX

### Abbreviations used

APF = after puparium formation

bp = base pair

cDNA = complimentary DNA

CtBP = C-terminal Binding Protein

dsDNA = double stranded DNA

EcR = Ecdysone Receptor

EtBr = Ethidium Bromide

JH = Juvenile hormone

RT = Reverse Transcriptase

RT-PCR = Reverse Transcriptase Polymerase Chain Reaction

PBS = 1x phosphate buffered saline

PCR = Polymerase Chain Reaction

PTTH = prothoracicotropic hormone

qPCR = quantitative Polymerase Chain Reaction

TAE = tris-acetate EDTA

USP = Ultraspiracle





**Table 13. A sample 96-well plate layout for the Experimental qPCR to determine gene expressions at 10 hours APF.** (1) = 1<sup>st</sup> source of cDNA, (2) = second source of cDNA,  $E93^I = E93^I/DF(3R)93F^{X2}$

	1	2	3	4	5	6	7	8	9	10	11	12
A	10 <sup>0</sup> <i>w</i> <sup>1118</sup> cDNA, <i>Actin</i> 5C	10 <sup>-1</sup> <i>w</i> <sup>1118</sup> cDNA, <i>Actin</i> 5C	10 <sup>-2</sup> <i>w</i> <sup>1118</sup> cDNA, <i>Actin</i> 5C	10 <sup>-3</sup> <i>w</i> <sup>1118</sup> cDNA, <i>Actin</i> 5C	10 <sup>-4</sup> <i>w</i> <sup>1118</sup> cDNA, <i>Actin</i> 5C		No-RT <i>w</i> <sup>1118</sup> cDNA, <i>Actin</i> 5C					
B												
C	10 <sup>0</sup> <i>w</i> <sup>1118</sup> cDNA, <i>MMP2</i>	10 <sup>-1</sup> <i>w</i> <sup>1118</sup> cDNA, <i>MMP2</i>	10 <sup>-2</sup> <i>w</i> <sup>1118</sup> cDNA, <i>MMP2</i>	10 <sup>-3</sup> <i>w</i> <sup>1118</sup> cDNA, <i>MMP2</i>	10 <sup>-4</sup> <i>w</i> <sup>1118</sup> cDNA, <i>MMP2</i>		No-RT <i>w</i> <sup>1118</sup> cDNA, <i>MMP2</i>					
D												
E	<i>w</i> <sup>1118</sup> , <i>Actin</i> 5C RT (1)	<i>w</i> <sup>1118</sup> , <i>Actin</i> 5C RT (2)	<i>w</i> <sup>1118</sup> , <i>MMP2</i> RT (1)	<i>w</i> <sup>1118</sup> , <i>MMP2</i> RT (2)	<i>w</i> <sup>1118</sup> , <i>Actin</i> 5C No-RT	<i>w</i> <sup>1118</sup> , <i>MMP2</i> No-RT						
F												
G	$E93^I$ , <i>Actin</i> 5C RT (1)	$E93^I$ , <i>Actin</i> 5C RT (2)	$E93^I$ , <i>MMP2</i> RT (1)	$E93^I$ , <i>MMP2</i> RT (2)	$E93^I$ , <i>Actin</i> 5C No-RT	$E93^I$ , <i>MMP2</i> No-RT						
H												

A sample Amplification plot generated using 7300 BioAnalyzer software for *Actin* 5C primers (300nm forward:100nm reverse) at 10 hours APF (*w*<sup>1118</sup> cDNA series dilutions = 260ng, 26ng, 2.6ng, 0.26ng and 0.026ng)

### Rate of Fluorescence versus Cycle Number

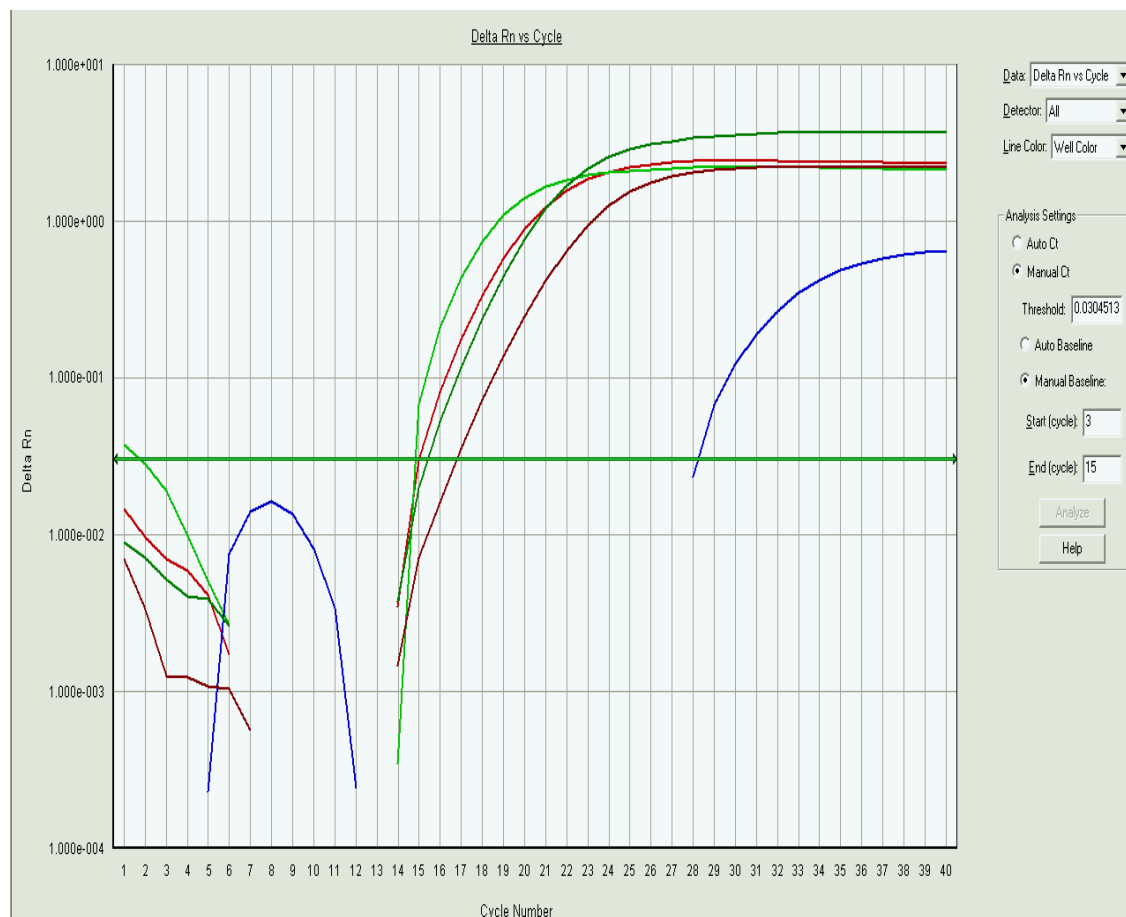


**Figure 12. Exponential curves for the different dilutions ranging from 0.026ng to 260ng of  $w^{1118}$  cDNA at 10 hours APF with *Actin 5C* primer set generated in the 7300 BioAnalyzer software.**

The lowest C<sub>t</sub> value indicates high gene expression. The cycle number at which the gene is amplified exponentially is known as the threshold value (C<sub>t</sub>). Each color is a representation of a cDNA dilution in the particular well.

A sample Amplification plot generated using 7300 BioAnalyzer software for *MMP2* primers (500nm forward: 500nm reverse) at 10 hours APF (w<sup>1118</sup> cDNA series dilutions = 260ng, 26ng, 2.6ng, 0.26ng and 0.026ng)

### Rate of Fluorescence versus Cycle Number



**Figure 13. Exponential curves for each w<sup>1118</sup> cDNA dilution (ranging from 0.026ng to 260ng) at 10 hours APF.**

## REFERENCES

- Alimonti, B.J., Ball, B.T., and Fowke, K.R., 2003. Mechanisms of CD4+ T lymphocyte cell death in human immunodeficiency virus infection and AIDS. *J Gen Virology*. 84(7):1649-61
- Baehrecke, E.H., Thummel, C.S., 1995. The *Drosophila* E93 gene from the 93F early puff displays stage- and tissue-specific regulation by 20-hydroxyecdysone. *Dev Biol*. 171(1),85-97
- Baehrecke, E.H., 2000. Steroid regulation of programmed cell death during *Drosophila* development. *Cell Death Differ*. 7,1057-1062
- Bainbridge, S.P., Bownes, M., 1981. Staging the metamorphosis of *Drosophila melanogaster*. *J. Embryol. Exp. Morph*. 66, 57-80.
- Bender, M., Imam, F.B., Talbot, W.S., Ganetzky, B., and Hogness, D.S., 1997. *Drosophila* ecdysone receptor mutations reveal functional differences among receptor isoforms. *Cell*. 91, 777-788.
- Bond, N.D., Nelliott, A., Bernado, M.K., Ayerh, M.A., Gorski, K.A., Hoshizak, D.K., Woodard, C.T., 2011.  $\beta$ FTZ-F1 and metalloproteinase 2 are required for fat body remodeling in *Drosophila*. *Developmental Biology*. 360,286-29.
- Brew, K., Dinakarpanian, D., and Nagase, H., 2000. Tissue inhibitors of metalloproteinases: evolution, structure and function. *Biochim Biophys Acta*. 1477,267-83.
- Broadus, J., McCabe, J., Endrizzi, B., Thummel, C.S., and Woodard, C.T., 1999. The *Drosophila* *Bftz-f1* orphan nuclear receptor provides competence for stage-specific responses to the steroid hormone ecdysone. *Mol.Cell*. 3,143-149.
- Chavez, V.M., Marques, G., Delbecque, J.P., Kobayashi, K., Hollingsworth, M., Burr, J., Natzle, J.E., and O'Connor, M.B., 2000. The *Drosophila* disembodied gene controls late embryonic morphogenesis and codes for a cytochrome P450 enzyme that regulates embryonic ecdysone levels. *Development*. 127(19), 4115-4126.

Cherbas, I., Hu, X., Zhuimulev, I., Belyaeva, E., Cherbas, P., 2003. EcR isoforms in *Drosophila*: Testing tissue-specific requirements by targeted blockade and rescue. *Development*. 130,271-284.

Di Bello, P.R., Winthers, D.A., Bayer, C.A., Fristrom, J.W., and Guild, G.M., 1991. The *Drosophila Broad Based-Complex* encodes a family of regulated proteins containing zinc fingers. *Genetics*. 129,385-397.

Egald, M., and Werb, Z., 2002. New functions for the matrix metalloproteinase in cancer progression. *Nat.Rev Cancer*. 2,161-174.

Evans-Storm, R.B., and Cidlowski, J.A., 1995. Regulation of apoptosis by steroid hormones. *J.Steroid Biochem.Mol.Biol*. 53,1-6.

Fortier, T.M., Vasa, P.P., and Woodard, C.T., 2003. Orphan nuclear receptor *Bftz-fl* is required for muscle-driven morphogenetic events at the prepupal-pupal transition in *Drosophila melanogaster*. *Dev Biol*. 257,153-65.

Godenschwege, T.A., Pohar, N., Buchner, E., 2000. Inflated wings, tissue autolysis and early death in tissue inhibitor of metalloproteinases mutants of *Drosophila*. *Eur.J.Cell Biol*. 79,495-501.

GomisRuth, F.X., Maskos, K., Betz, M., Bergner, A., Huber, R., Suzuki, K., Yoshida, N., Nagase, H., Brew, K., Bourenkov, G.P et al., 1997. Mechanism of inhibition of human matrix metalloproteinase stromelysin-1 by TIMP-1. *Nature*. 389,77-81.

Goni, R., Garcia, P., and Sylvain, F., 2009. The qPCR data statistical analysis. *Integromics SL*. 1-9.

Heery, D.M., Kalhoven, E., Hoare, S., and Parker, M.G., 1997. A signature motif in transcriptional co-activators mediates binding to nuclear receptors. *Nature*. 387,733-736

Heffner, L.J., Schust, D.J., 2010. The Reproductive System at a Glance. *John Wiley and Sons*. pp. 16.

- Jacobsen, M.D., Weil, M., and Raff, M.C., 1997. Programmed cell death in animal development. *Cell*. 88,347-354.
- Jiang, C., Baehrecke, E.H., and Thummel, C.S., 1997. Steroid regulated programmed cell death during *Drosophila* metamorphosis. *Development*. 124,4673-4683.
- King-Jones, K., and Thummel, C.S., 2005. Nuclear receptors-A perspective from *Drosophila*. *Nat Rev Genet*.6,311-323.
- Koelle, M.R., Talbot, W.S., Seagraves, W.A., Bender, M.T., Cherbas, P., and Hognes, D.S., 1991. The *Drosophila* EcR gene encodes an ecdysone receptor, a new member of the steroid receptor superfamily. *Cell*.67,59-77.
- Krammer, P.H., 2000. CD95's deadly mission in the immune system. *Nature*. 407,789-795.
- Lee, C., Wendel, D.P., Reid, P., Lam, G., Thummel, C. S., Baehrecke E. H., 2000. *E93* Directs Steroid-Triggered Programmed Cell Death in *Drosophila*. *Molecular Cell*. Vol 6, 433-443.
- Lee, C.Y., and Baehrecke, E.H., 2001. Steroid regulation of autophagic programmed cell death in *Drosophila*. *Mol.Cell*. 6,433-443.
- Livak, K. J., and Schmittgen T.D., 2001. Analysis of relative gene expression data using real-time quantitative PCR and the 2(-Delta Delta C(T)) Method. *Methods* (San Diego, Calif.) 25, no. 4 (December), 402-408.
- Llano, E., Pendas, A.M., Aza-Blanc, P., Komberg, T.B., and Lopez-Otin, C., 2000. Dm1-MMP, a matrix metalloproteinase from *Drosophila* with a potential role in extracellular matrix remodeling during neural development. *J.Biol.Chem*. 274, 34706-34710.
- Llano, E., Adam, G., Pendas, A.M., Quesada, V., Sanchez, L.M., Santamaria, I., Noselli, S., and Lopez-Otin, C., 2002. Structural and enzymatic characterization of *Drosophila* Dm2-MMP, a membrane-bound matrix metalloproteinase with tissue-specific expression. *J.Biol. Chem*. 277, 23321-23329.

Lockshin, R.A., and Zakeri, Z., 1991. Programmed cell death and apoptosis. In "Apoptosis: the Molecular Basis of Cell Death" (L.D. Tomei and F.O. Cope, Eds). Cold Spring Harbor Laboratory Press, Cold Spring Harbor, NY. Vol.3. pp47-60

McCawley, L.J., and Matrisian, L.M., 2001. Matrix metalloproteinases: they're not just for matrix anymore! *Curr. Opin. Cell Biol.* 13, 534-540.

Nelliot, A., Bond, N., and Hoshizaki, D.K., 2006. Fat-body remodeling in *Drosophila melanogaster*. *Genesis*. 44, 396-400.

Page-McCaw, A., Serano, J., Sante, J.M., Rubin, G.M., 2003. *Drosophila* matrix metalloproteinases are required for tissue remodeling, but not embryonic development. *Dev. Cell.* 4, 95-106.

Page-McCaw, A., Ewald, A.J., Werb, Z., 2007. Matrix metalloproteinases and the regulation of tissue remodeling. *Nat. Rev. Mol. Cell Bio.* 8, 221-233.

Riddiford, L.M., 1993. Hormones and *Drosophila* development. In *The Development of Drosophila melanogaster*, Ed. Bate M. Arias AM. Cold Spring Harbor Laboratory Press. 2, 899-939.

Riddiford, L.M., 2008. Juvenile hormone action: a 2007 perspective. *J Insect Physiol.* 54, 895-901.

Siegmund, T., Lehmann, M., 2002. The *Drosophila* Pipsqueak protein defines a new family of helix-turn-helix DNA-binding proteins. *Dev Genes Evol.* 212, 152-157.

Sternlich, M.D., and Werb, Z., 2001. How matrix metalloproteinases regulate cell behavior. *Annu. Rev. Cell Dev. Biol.* 17, 463-516.

Stone, A.L., Kroeger, M., Sang, Q.X., 1999. Structure-function analysis of the ADAM family of disintegrin-like and metalloproteinase-containing proteins (review). *J Protein Chem.* 18(4), 447-65.



- Talbot, W.S., Swyryd, E.A., and Hogness, D.S., 1993. *Drosophila* tissues with different metamorphic responses to ecdysone express different ecdysone receptor isoforms. *Cell*. 73, 1323-37.
- Thomas, H.E., Stunnenberg, H.G., and Stewart, A.F., 1993. Heterodimerization of the *Drosophila* ecdysone receptor with retinoid X receptor and ultraspiracle. *Nature*. 362, 471-475
- Thummel, C.S., 1996. Flies on steroids: *Drosophila* metamorphosis and the mechanisms of steroid hormone action. *Trends Genet*. 12, 306-310.
- Vaux, D.L., and Korsmeyer, S.J., 1999. Cell death in development. *Cell*. 96, 245-254
- Vo, N., Fjeld, C., and Goodman, R.H., 2001. Acetylation of nuclear hormone receptor-interacting protein RIP140 regulates binding of the transcriptional corepressor CtBP. *Mol Cell Biol*. 21, 6181-6188.
- Wei, S., Xie, Z., Filenova, E., and Brew, K., 2003. *Drosophila* TIMP is a potent inhibitor of MMPs and TACE: similarities in structure and function to TIMP-3. *Biochemistry*. 42, 12200-12207.
- Woodard, C.T., Baehrecke, E.H., and Thummel, C.S., 1994. A molecular mechanism for the stage-specificity of the *Drosophila* prepupal genetic response to ecdysone. *Cell*. 79, 607-615.
- Xiachun, M., Dianne, M.D., Baehrecke, H.E., and Duncan, I., 2012. Control of target gene specificity during metamorphosis by the steroid response gene *E93*. *PNAS*. Vol. 109.no.8. 2949-2954.
- Yamanda, M., Murata, T., Hirose, S., Lavorgna, G., Suzuki, E., and Ueda, H., 2000. Temporally restricted expression of transcription factor  $\beta$ FTZ-F1: Significance for embryogenesis, molting, and metamorphosis in *Drosophila melanogaster*. *Development* .127, 5083-5092.
- Yao, T.P., Segraves, W.A., Oro, A.E., McKeown, M., and Evans, R.M., 1992. *Drosophila* ultraspiracle modulates ecdysone receptor function via heterodimer formation. *cell*. 71, 63-72.

Yorimitsu, T., and Klionsky, D.J., 2005. Autophagy: molecular machinery for self-eating. *Cell death and Differentiation*. 12, 1542-1552.

Yuan, J., and Yanker, B.A., 2000. Apoptosis in the nervous system. *Nature*. 407, 802-809

Zhou, X., Riddiford, L.M., 2002. Broad specifies pupal development and mediates the 'status quo' action of juvenile hormone on the pupal-adult transformation in *Drosophila* and *Manduca*. *Development*. 129(9), 2259-2269.